Mon. Not. R. Astron. Soc. **386,** 2115–2134 (2008) doi:10.1111/j.1365-2966.2008.13181.x

The luminosities and distance scales of type II Cepheid and RR Lyrae variables

Michael W. Feast,[1⋆] Clifton D. Laney,[2] Thomas D. Kinman,[3] Floor van Leeuwen[4] and Patricia A. Whitelock[1,2,5]

[1]*Astronomy Department, University of Cape Town, 7701 Rondebosch, South Africa*
[2]*South African Astronomical Observatory, PO Box 9, 7935 Observatory, South Africa*
[3]*National Optical Astronomy Observatory, Tucson, PO Box 26732, AZ 85726, USA*
[4]*Institute of Astronomy, Madingley Road, Cambridge CB3 0HA*
[5]*National Astrophysics and Space Science Programme, Department of Mathematics and Applied Mathematics, University of Cape Town, 7701, South Africa*

Accepted 2008 February 29. Received 2008 February 29; in original form 2008 January 26

ABSTRACT

Infrared and optical absolute magnitudes are derived for the type II Cepheids κ Pav and VY Pyx using revised *Hipparcos* parallaxes and for κ Pav, V553 Cen and SW Tau from pulsational parallaxes. Revised *Hipparcos* and *HST* parallaxes for RR Lyrae agree satisfactorily and are combined in deriving absolute magnitudes. Phase-corrected J, H and K_s mags are given for 142 *Hipparcos* RR Lyraes based on Two-Micron All-Sky Survey observations. Pulsation and trigonometrical parallaxes for classical Cepheids are compared to establish the best value for the projection factor (p) used in pulsational analyses.

The M_V of RR Lyrae itself is 0.16 ± 0.12 mag brighter than predicted from an M_V–[Fe/H] relation based on RR Lyrae stars in the Large Magellanic Cloud (LMC) at a modulus of 18.39 ± 0.05 as found from classical Cepheids. This is consistent with the prediction of Catelan & Cortés that it is overluminous for its metallicity. The M_{K_s} results for the metal- and carbon-rich Galactic disc stars, V553 Cen and SW Tau, each with small internal errors (± 0.08 mag) have a mean deviation of only 0.02 mag from the period–luminosity (PL) relation established by Matsunaga et al. for type II Cepheids in globular clusters and with a zero-point based on the same LMC-scale. Comparing directly the luminosities of these two stars with published data on type II Cepheids in the LMC and in the Galactic bulge leads to an LMC modulus of 18.37 ± 0.09 and a distance to the Galactic Centre of $R_0 = 7.64 \pm 0.21$ kpc. The data for VY Pyx agree with these results within the uncertainties set by its parallax. Evidence is presented that κ Pav may have a close companion and possible implications of this are discussed. If the pulsational parallax of this star is incorporated in the analyses, the distance scales just discussed will be increased by $\sim 0.15 \pm 0.15$ mag. V553 Cen and SW Tau show that at optical wavelengths PL relations are wider for field stars than for those in globular clusters. This is probably due to a narrower range of masses in the latter case.

Key words: stars: distances – Cepheids – Magellanic Clouds – distance scale.

1 INTRODUCTION

The RR Lyrae variables are known, primarily from studies of globular clusters, to lie on or immediately above the horizontal branch (HB) in an Hertzsprung–Russell (HR) diagram. Globular cluster studies also show a class of variable stars lying in an instability strip in an HR diagram which extends approximately 3 mag above the HB. Variables with similar characteristics are also found in the general field, both in the halo and in the disc. All these variables, both in clusters and the field are classified together as 'type II Cepheids' (CephIIs). These stars have been divided into three classes according to their periods. Those of short period (roughly $P < 7$ d) are called BL Her stars, whilst longer period ones (up to $P \sim 20$ d) are called W Vir stars. At even longer periods, many of the CephIIs show characteristic alternations of deep and shallow minima and are classified as RV Tau stars. This subdivision of CephIIs has not been universally adopted. Thus, Sandage & Tammann (2006) review and

⋆E-mail: mwf@artemisia.ast.uct.ac.za

summarize a system of classification based on light curve parameters that relate to their population characteristic and these partially correlate with their metallicities. It should be noted that the 'Population II Cepheids' with which Sandage & Tammann are primarily concerned are a subset of the 'CephIIs'. Maas, Giridhar & Lambert (2007) have shown that the shorter period CephIIs in the general field differ from those of longer period in their detailed chemical composition. The short-period stars are generally believed (Gingold 1976, 1985) to be evolving across the instability strip from the HB towards the asymptotic giant branch (AGB). The longer period stars, on the other hand, are believed to be on blueward excursions into the instability strip from the AGB due to shell flashing.

In this paper, we discuss the luminosities of RR Lyraes and CephIIs on the basis of the revised *Hipparcos* trigonometrical parallaxes (van Leeuwen 2007a, see also van Leeuwen 2007b) and newly derived pulsational parallaxes for three CephII variables.

2 PERIOD–LUMINOSITY AND METALLICITY–LUMINOSITY RELATIONS

Here, we present various relations which are required in the interpretation of our data.

2.1 Relationships for RR Lyrae variables

It has long been thought that the luminosities of RR Lyrae variables can be expressed in the form

$$M_V = a[\mathrm{Fe/H}] + b. \tag{1}$$

However, the values of *a* and *b* have been much disputed, as has the question of the linearity of the equation. In the following, we adopt

$$M_V = 0.214[\mathrm{Fe/H}] + [19.39 - \mathrm{Mod(LMC)}]. \tag{2}$$

This is based on RR Lyraes in the Large Magellanic Cloud (LMC) (Gratton et al. 2004). Adopting an LMC modulus of 18.39[1] as derived from classical Cepheids (Benedict et al. 2007; van Leeuwen et al. 2007), the constant term becomes

$$b = +1.0.$$

The LMC RR Lyraes, on which this relation is based, cover a range in [Fe/H] from ~ -0.8 to -2.2, but are mainly concentrated between -1.3 and -1.8. There is evidence, however, that the slope of the relation is not universal. Clementini et al. (2005) find that in the Sculptor dwarf spheroidal, over roughly the same metallicity range, the slope is 0.092 ± 0.027 compared with the LMC 0.214 ± 0.047 and they suggest that the Sculptor RR Lyraes are on average more evolved than those in the LMC.

That there is a period–luminosity (PL) relation for RR Lyraes in the *K* band [PL(*K*)], possibly independent, or nearly independent of metallicity, goes back at least to the work of Longmore, Fernley & Jameson (1986) on globular clusters. The most recent version of such a relation was given by Sollima, Cacciari & Valenti (2006) again based on globular clusters. The relative distances of the clusters came from main-sequence fitting and the zero-point of their final relation was set by a trigonometrical parallax of RR Lyrae itself (Benedict et al. 2002a). They found

$$M_{K_s} = -2.38(\pm0.04)\log P + 0.08(\pm0.11)[\mathrm{Fe/H}] - 1.05(\pm0.13), \tag{3}$$

where K_s is the K_s magnitude in the Two-Micron All-Sky Survey (2MASS) system. The term in [Fe/H] is small and not statistically significant.

2.2 Relationships for type II Cepheids

In the past, various PL relations for CephIIs at visual wavelengths have been suggested based primarily on globular cluster work. More recently, it was shown from globular cluster data that a well-defined PL(K_s) relation, with small scatter, applied (Matsunaga et al. 2006). The globular cluster distances were determined from a relation for HB stars similar to equation (2) and we may write the Matsunaga CephII relation as

$$M_{K_s} = -2.41(\pm0.05)\log P + c, \tag{4}$$

where $c = 17.39 - \mathrm{Mod(LMC)}$ and $c = -1.0$ for Mod(LMC) = 18.39 as above. The (internal) standard error of the constant term is ±0.02 at the mean $\log P$ (1.120). Matsunaga et al. pointed out that RR Lyraes in clusters lay on an extrapolation of this relation to shorter periods. The subsequent work of Sollima et al. (2006) confirms this (compare equations 3 and 4). Matsunaga et al. examined their data for a metallicity effect on the PL(*K*) zero-point and found a term, -0.10 ± 0.06. This is clearly not significant and is of opposite sign to the metallicity term in the RR Lyrae relation, equation (3), which is also not significant. This suggests that a combined RR Lyrae/CephII PL(*K*) is virtually metal-independent in globular clusters. Some caution is necessary in accepting this, however, since there are only four CephIIs in the Matsunaga sample with $[\mathrm{Fe/H}] > -1.0$ and these all have periods greater than 10 d.[2]

In addition to the above, the following three PL relations at optical wavelengths will be required later. They are based on CephIIs in NGC 6441 and NGC 6388 and are taken directly from Pritzl et al. (2003):

$$M_V = -1.64(\pm0.05)\log P + 0.05(\pm0.05), \tag{5}$$

$$M_B = -1.23(\pm0.09)\log P + 0.31(\pm0.09), \tag{6}$$

$$M_I = -2.03(\pm0.03)\log P - 0.36(\pm0.01). \tag{7}$$

3 THE RR LYRAE VARIABLES

3.1 Data

Table 1 lists the data for 142 RR Lyrae variables.

The stars are those listed by Fernley et al. (1998) and we have generally adopted their *V* magnitudes and [Fe/H] values. The parallaxes and their standard errors are from the revised *Hipparcos* catalogue (van Leeuwen 2007a). Details regarding the formation of the table, particularly the derivation of mean JHK_s values from the single 2MASS values, are given in Appendix B.[3] DH Peg, which is in the Fernley et al. list, has been omitted because its status is

[1] This includes a correction for metallicity effects based on Macri et al. (2006).

[2] But see the discussion of the field variables below.

[3] Since our analysis of the RR Lyrae data was completed, Sollima et al. (2008) have published mean *J*, *H* and K_s data for RR Lyrae itself. They measured against 2MASS stars as standards and found 6.74 ± 0.02, 6.60 ± 0.03 and 6.50 ± 0.02. The values we derived (Table 1) are 6.76, 6.55 and 6.49. The Sollima et al. results provide a useful confirmation of our procedure. Since their value of K_s is negligibly different from our value, we have kept our value in the following.

Table 1. Basic data used in the analysis.

Hipparcos	Name	π (mas)	$\Delta\pi$ (mas)	V (mag)	J (mag)	H (mag)	K_s (mag)	P (d)	[Fe/H]	$E(B-V)$ (mag)	Type
226	RU Scl	0.99	1.96	10.220	9.474	9.294	9.229	0.493 347	−1.27	0.018	
320	UU Cet	1.59	5.73	12.080	11.137	10.863	10.837	0.606 080	−1.28	0.021	
1878	SW And	−0.01	1.84	9.710	8.809	8.578	8.505	0.442 262	−0.24	0.038	
2655	RX Cet	3.24	4.74	11.440	10.606	10.378	10.319	0.573 685	−1.28	0.025	
4541	W Tuc	5.37	2.41	11.410	10.594	10.373	10.344	0.642 260	−1.57	0.021	
4725	RU Cet	7.14	4.62	11.680	10.597	10.487	10.465	0.586 267	−1.66	0.023	
5803	RU Psc	1.30	2.08	10.190	9.347	9.162	9.117	0.390 333	−1.75	0.043	c
6029	XX And	−0.79	2.50	10.680	9.727	9.488	9.409	0.722 755	−1.94	0.039	
6094	VW Scl	2.34	2.79	11.030	10.418	10.193	10.136	0.510 913	−0.84	0.016	
6115	AM Tuc	−1.93	2.28	11.670	10.865	10.617	10.563	0.405 769	−1.49	0.023	c
7149	RR Cet	0.48	1.85	9.730	8.829	8.623	8.520	0.553 030	−1.45	0.022	
7398	VX Scl	3.71	3.64	12.020	11.094	10.894	10.853	0.637 058	−2.25	0.014	
8163	SV Scl	5.50	2.37	11.380	10.718	10.596	10.543	0.377 380	−1.77	0.014	c
8939	CI And	0.77	5.87	12.280	11.182	11.018	11.185	0.484 728	−0.69	0.062	
9932	SS For	3.57	1.98	10.190	9.546	9.305	9.246	0.495 424	−0.94	0.014	
10491	RV Cet	2.16	2.70	10.920	9.903	9.580	9.520	0.623 350	−1.60	0.024	
11517	RZ Cet	−0.04	4.92	11.850	11.031	10.787	10.737	0.510 606	−1.36	0.029	
12199	CS Eri	2.70	1.10	9.000	8.144	8.014	7.973	0.311 332	−1.41	0.018	c
14601	X Ari	0.99	1.90	9.570	8.365	8.042	7.941	0.651 154	−2.43	0.180	
14856	SV Eri	3.18	2.53	9.960	8.958	8.710	8.642	0.713 865	−1.70	0.085	
16321	SX For	−5.39	2.38	11.120	10.035	9.847	9.772	0.605 342	−1.66	0.012	
19993	AR Per	−1.32	2.02	10.510	9.012	8.710	8.642	0.425 551	−0.30	0.108	
22442	RX Eri	1.31	1.70	9.690	8.737	8.485	8.429	0.587 246	−1.33	0.058	
22466	U Pic	3.21	2.21	11.380	10.689	10.464	10.381	0.440 373	−0.72	0.009	
22750	BB Eri	5.44	3.58	11.520	10.321	10.147	10.110	0.569 909	−1.32	0.048	
22952	U Lep	2.32	2.97	10.570	9.814	9.565	9.542	0.581 479	−1.78	0.027	
24471	RY Col	3.35	1.79	10.900	10.254	9.732	9.699	0.478 832	−0.91	0.026	
29528	RX Col	−4.02	5.53	12.720	11.634	11.393	11.313	0.593 780	−1.70	0.082	
34743	TZ Aur	−3.70	6.39	11.910	10.975	10.771	10.731	0.391 676	−0.79	0.037	
35281	AA CMi	1.40	5.22	11.570	10.570	10.384	10.281	0.476 327	−0.15	0.011	
35584	HH Pup	2.39	2.53	11.290	10.248	10.044	9.975	0.390 748	−0.50	0.158	
35667	RR Gem	0.43	3.24	11.380	10.566	10.306	10.275	0.397 292	−0.29	0.054	
37779	HK Pup	−2.90	3.60	11.370	10.240	10.010	9.915	0.734 229	−1.11	0.160	
37805	TW Lyn	−6.62	8.60	12.000	11.075	10.854	10.778	0.481 862	−0.66	0.051	
38561	SZ Gem	6.04	4.19	11.750	11.072	10.798	10.748	0.501 143	−1.46	0.013	
39009	UY Cam	0.19	1.99	11.530	11.002	10.872	10.859	0.267 044	−1.33	0.022	c
39849	XX Pup	−0.15	3.81	11.250	10.321	10.118	10.084	0.517 203	−1.33	0.068	
40186	DD Hya	−5.41	5.88	12.220	11.457	11.241	11.228	0.501 771	−0.97	0.013	
41936	TT Cnc	2.42	5.55	11.350	10.330	10.047	9.968	0.563 430	−1.57	0.043	
44428	TT Lyn	−1.48	1.75	9.860	8.908	8.655	8.611	0.597 429	−1.56	0.017	
45709	RW Cnc	1.05	4.98	11.850	10.677	10.561	10.530	0.547 224	−1.67	0.020	
48503	T Sex	2.24	1.56	10.040	9.438	9.268	9.200	0.324 706	−1.34	0.044	c
49628	RR Leo	5.01	3.16	10.730	10.021	9.778	9.730	0.452 392	−1.60	0.037	
50073	WZ Hya	4.50	5.17	10.900	9.945	9.669	9.610	0.537 713	−1.39	0.075	
50289	WY Ant	−0.27	2.51	10.870	9.970	9.744	9.674	0.574 341	−1.48	0.059	
53213	AF Vel	0.57	3.19	11.440	10.354	10.079	10.040	0.527 414	−1.49	0.250	
55825	W Crt	−1.95	3.43	11.540	10.774	10.590	10.539	0.412 015	−0.54	0.040	
56088	TU UMa	0.56	1.68	9.820	8.919	8.740	8.660	0.557 658	−1.51	0.022	
56350	AX Leo	−3.10	7.00	12.260	11.302	11.048	10.951	0.726 845	−1.72	0.033	
56409	SS Leo	2.50	4.01	11.030	10.259	10.008	9.943	0.626 335	−1.79	0.018	
56734	SU Dra	1.27	1.53	9.780	8.898	8.676	8.619	0.660 418	−1.80	0.010	
56742	BX Leo	7.73	6.17	11.610	10.889	10.743	10.709	0.362 757	−1.28	0.023	c
56785	ST Leo	−0.45	3.47	11.490	10.690	10.480	10.446	0.477 990	−1.17	0.038	
57625	X Crt	−3.98	4.50	11.480	10.482	10.213	10.148	0.732 842	−2.00	0.027	
58907	IK Hya	1.39	1.62	10.110	9.144	8.863	8.760	0.650 371	−1.24	0.061	
59208	UU Vir	2.24	2.91	10.560	9.596	9.436	9.414	0.475 597	−0.87	0.018	
59411	AB UMa	0.12	1.94	10.940	9.934	9.678	9.623	0.599 593	−0.49	0.022	
59946	SW Dra	2.24	1.42	10.480	9.594	9.362	9.319	0.569 671	−1.12	0.014	
61029	UZ CVn	6.50	7.59	12.120	11.219	10.941	10.885	0.697 791	−1.89	0.019	
61031	SV Hya	3.79	2.16	10.530	9.673	9.455	9.366	0.478 542	−1.50	0.080	
61225	S Com	5.16	3.66	11.630	10.823	10.678	10.619	0.586 585	−1.91	0.019	
61809	U Com	7.40	4.05	11.740	11.186	10.984	10.987	0.292 736	−1.25	0.014	c

Table 1 – *continued*

Hipparcos	Name	π (mas)	$\Delta\pi$	V	J (mag)	H	K_s	P (d)	[Fe/H]	$E(B-V)$ (mag)	Type
63054	AT Vir	1.32	3.03	11.340	10.547	10.363	10.332	0.525 785	−1.60	0.030	
64875	ST Com	−3.68	3.55	11.460	10.461	10.258	10.186	0.598 927	−1.10	0.024	
65063	AV Vir	2.22	4.73	11.820	10.853	10.615	10.566	0.656 910	−1.25	0.028	
65344	AM Vir	−1.79	3.17	11.520	10.509	10.253	10.199	0.615 063	−1.37	0.067	
65445	AU Vir	0.06	4.99	11.590	11.085	10.918	10.847	0.339 616	−1.50	0.028	c
65547	SX UMa	1.90	1.81	10.840	10.288	10.135	10.071	0.307 139	−1.81	0.010	c
66122	RV UMa	−0.30	1.85	10.770	10.058	9.854	9.831	0.468 069	−1.20	0.018	
67087	RZ CVn	−2.03	2.99	11.570	10.733	10.518	10.478	0.567 403	−1.84	0.014	
67227	RV Oct	1.75	2.17	10.980	9.879	9.614	9.526	0.571 169	−1.71	0.180	
67354	SS CVn	2.14	3.83	11.840	11.185	10.951	10.936	0.478 510	−1.37	0.006	
67976	V499 Cen	−0.01	2.97	11.120	10.225	9.926	9.922	0.521 205	−1.43	0.085	
68188	ST CVn	−1.28	4.11	11.370	10.626	10.459	10.449	0.329 065	−1.07	0.012	c
68292	UY Boo	1.45	3.00	10.940	9.981	9.755	9.723	0.650 889	−2.56	0.033	
68908	W CVn	2.95	2.42	10.550	9.667	9.454	9.371	0.551 753	−1.22	0.005	
69759	TV Boo	−0.05	2.09	10.970	10.373	10.282	10.248	0.312 557	−2.44	0.010	c
70702	ST Vir	−5.10	5.66	11.520	10.914	10.748	10.671	0.410 806	−0.67	0.039	
70751	AF Vir	−9.08	5.23	11.800	10.939	10.769	10.684	0.483 735	−1.33	0.023	
71186	RS Boo	1.62	1.91	10.370	9.744	9.559	9.507	0.377 339	−0.36	0.012	
72115	TW Boo	−2.23	2.28	11.290	10.407	10.192	10.170	0.532 277	−1.46	0.013	
72342	AE Boo	0.33	2.00	10.650	9.974	9.819	9.762	0.314 893	−1.39	0.023	c
72444	TY Aps	1.78	3.07	11.850	10.819	10.532	10.456	0.501 695	−0.95	0.169	
72691	BT Dra	−1.26	2.08	11.640	10.735	10.478	10.397	0.588 673	−1.75	0.010	
72721	XZ Aps	−4.19	5.48	12.380	11.284	11.006	10.923	0.587 275	−1.06	0.135	
74556	AP Ser	−0.16	4.32	11.110	10.462	10.305	10.268	0.340 805	−1.58	0.042	c
75225	TV CrB	1.89	5.75	11.870	11.037	10.814	10.774	0.584 629	−2.33	0.033	
75234	FW Lup	1.58	1.18	9.060	7.995	7.836	7.671	0.484 169	−0.20	0.077	
75942	ST Boo	−0.13	1.80	11.010	10.185	9.981	9.930	0.622 286	−1.76	0.021	
75982	VY Ser	−0.77	1.99	10.130	9.205	8.944	8.826	0.714 101	−1.79	0.040	
76313	CG Lib	−0.50	5.67	11.550	10.437	10.208	10.125	0.306 787	−1.19	0.297	c
77663	VY Lib	−1.84	4.04	11.730	10.480	10.174	10.070	0.533 941	−1.34	0.192	
77830	AN Ser	−4.47	4.79	10.940	10.096	9.898	9.842	0.522 069	−0.07	0.040	
77997	AT Ser	0.18	5.30	11.480	10.533	10.248	10.214	0.746 570	−2.03	0.037	
78417	AR Her	2.08	3.25	11.240	10.605	10.413	10.391	0.469 981	−1.30	0.013	
79974	RV CrB	3.77	3.21	11.410	10.555	10.418	10.336	0.331 593	−1.69	0.039	c
80402	V445 Oph	5.60	5.33	11.050	9.649	9.401	9.262	0.397 023	−0.19	0.287	
80853	VX Her	−0.78	2.65	10.690	9.848	9.651	9.590	0.455 362	−1.58	0.044	
80990	UV Oct	2.32	1.12	9.500	8.592	8.362	8.297	0.542 587	−1.74	0.091	
81238	RW Dra	1.38	2.44	11.710	10.779	10.596	10.622	0.442 909	−1.55	0.011	
83244	RW TrA	5.74	3.19	11.400	10.375	10.111	10.059	0.374 039	−0.13	0.105	
84233	VZ Her	3.49	2.12	11.480	10.746	10.590	10.496	0.440 331	−1.02	0.027	
87681	TW Her	−3.36	2.22	11.280	10.528	10.322	10.239	0.399 599	−0.69	0.042	
87804	WY Pav	1.08	6.99	12.180	10.836	10.647	10.553	0.588 573	−0.98	0.126	
88064	S Ara	−2.11	3.31	10.780	9.867	9.601	9.560	0.451 879	−0.71	0.124	
88402	MS Ara	8.81	5.20	12.070	11.036	10.763	10.664	0.524 982	−1.48	0.146	
89326	V675 Sgr	−1.28	2.75	10.330	9.313	9.053	9.003	0.642 280	−2.28	0.130	
89372	BC Dra	1.51	1.99	11.600	10.435	10.172	10.096	0.719 590	−2.00	0.068	
89450	V455 Oph	−1.47	6.69	12.360	11.395	11.160	11.088	0.453 882	−1.07	0.144	
90053	IO Lyr	−0.84	2.95	11.850	10.841	10.591	10.538	0.577 121	−1.14	0.074	
91634	CN Lyr	−3.91	2.52	11.480	10.282	10.055	9.919	0.411 383	−0.58	0.178	
92244	V413 CrA	−1.75	3.26	10.600	9.497	9.248	9.148	0.589 343	−1.26	0.075	
93476	MT Tel	1.17	1.46	8.980	8.323	8.176	8.076	0.316 900	−1.85	0.038	c
94134	XZ Dra	2.28	1.20	10.250	9.398	9.221	9.148	0.476 497	−0.79	0.062	
94869	BK Dra	0.67	1.52	11.190	10.336	10.124	10.071	0.592 076	−1.95	0.052	
95497	RR Lyr	3.79	0.19	7.760	6.759	6.546	6.489	0.566 839	−1.39	0.030	
95702	BN Vul	3.56	3.08	11.020	9.138	8.793	8.677	0.594 138	−1.61	0.173	
96101	V440 Sgr	−0.09	3.43	10.340	9.402	9.153	9.082	0.477 479	−1.40	0.085	
96112	XZ Cyg	1.83	1.01	9.680	8.990	8.793	8.722	0.466 610	−1.44	0.096	
96581	BN Pav	6.43	6.05	12.600	11.593	11.344	11.279	0.567 117	−1.32	0.073	
98265	BP Pav	3.50	6.34	12.540	11.648	11.386	11.366	0.527 128	−1.48	0.059	
101356	V341 Aql	−4.86	5.62	10.850	9.886	9.687	9.606	0.578 017	−1.22	0.086	
102593	DX Del	0.40	1.94	9.940	9.048	8.746	8.685	0.472 619	−0.39	0.092	
103364	UY Cyg	2.55	2.91	11.110	10.060	9.805	9.777	0.560 714	−0.80	0.129	

Table 1 – *continued*

Hipparcos	Name	π (mas)	$\Delta\pi$	V	J (mag)	H	K_s	P (d)	[Fe/H]	$E(B-V)$ (mag)	Type
103755	RV Cap	0.85	3.82	11.040	9.703	9.717	9.753	0.447 698	−1.61	0.041	
104613	V Ind	1.09	2.06	9.960	9.274	9.028	8.985	0.479 604	−1.50	0.043	
104930	SW Aqr	−3.93	4.09	11.180	10.413	10.142	10.057	0.459 299	−1.63	0.076	
105026	Z Mic	0.69	3.53	11.650	10.478	10.179	10.112	0.586 925	−1.10	0.094	
105285	YZ Cap	4.62	2.78	11.300	10.532	10.437	10.429	0.273 461	−1.06	0.063	c
106645	SX Aqr	2.42	3.58	11.780	10.973	10.689	10.639	0.535 712	−1.87	0.048	
106649	RY Oct	−1.87	4.88	12.060	11.118	10.917	10.859	0.563 475	−1.83	0.113	
107078	CG Peg	3.16	2.49	11.180	10.216	10.007	9.970	0.467 133	−0.50	0.074	
107935	AV Peg	2.88	2.44	10.500	9.609	9.406	9.346	0.390 378	−0.08	0.067	
108057	SS Oct	9.09	3.32	11.910	10.041	9.835	9.752	0.621 852	−1.60	0.285	
108839	BV Aqr	7.24	4.15	10.900	10.228	10.017	10.075	0.363 653	−1.42	0.034	
111839	RZ Cep	0.60	1.48	9.470	8.168	7.959	7.883	0.308 688	−1.77	0.078	c
112994	BH Peg	−0.72	2.38	10.460	9.385	9.114	9.067	0.640 991	−1.22	0.077	
115135	DN Aqr	−1.08	2.82	11.200	10.158	9.934	9.900	0.633 757	−1.66	0.025	
115870	RV Phe	1.75	4.71	11.940	11.106	10.828	10.768	0.59416	−1.69	0.007	
116664	BR Aqr	0.71	3.48	11.420	10.648	10.421	10.370	0.481 872	−0.74	0.027	
116942	VZ Peg	4.89	3.75	11.900	11.219	11.059	11.010	0.306 493	−1.80	0.045	c
116958	AT And	−2.25	1.85	10.710	9.478	9.181	9.087	0.616 917	−1.18	0.110	

doubtful. It may be a dwarf Cepheid (Fernley et al. 1990). There are a number of other stars which are listed as RR Lyrae stars in the *Hipparcos* catalogue. In some cases, this classification is incorrect or doubtful. For instance, DX Cet is actually a δ Sct star (Kiss et al. 1999). This star is, in fact, of special interest as having a parallax with a small percentage error and falling on the PL relation for fundamental mode δ Sct pulsators (van Leeuwen 2007a). A discussion of stars whose classification as RR Lyrae type is probably incorrect or uncertain will be given elsewhere (Kinman, in preparation). The parallaxes and magnitudes of the very few *Hipparcos* stars which are probably RR Lyraes and were not in the Fernley list are such that they would make no significant contribution to the results given in this paper. It seemed better therefore to omit them and thus, for instance, have the homogeneous set of [Fe/H] results given by Fernley et al. The reddenings, $E(B-V)$, listed are the means of the two values discussed in Section 3.2. These two values agree closely, the maximum difference (0.06 mag) being that for BN Vul, a star at low Galactic latitude. For RZ Cep, which is also close to the plane, the difference is 0.03 mag. All other stars show smaller differences.

We assume in the following that

$$A_V = 3.06\,E(B-V)$$

and with data on the 2MASS system we adopt

$$A_J = 0.764\,E(B-V),$$
$$A_H = 0.450\,E(B-V),$$
$$A_{K_s} = 0.285\,E(B-V).$$

These values are from Laney & Stobie (1993) as adjusted for K_s by Gieren, Fouqué & Gomez (1998). The table indicates the c-type variables. The fundamental periods of these stars were obtained by multiplying the observed period by 1.342.

3.2 Results

The revised *Hipparcos* parallax of RR Lyrae is $\pi = 3.46 \pm 0.64$. Benedict et al. (2002a) found $\pi = 3.82 \pm 0.20$ from *HST* observations. In this paper, we adopt a weighted mean of these values, $\pi = 3.79 \pm 0.19$. This takes the quoted standard errors, each of which has their own uncertainties, at their face value. Giving higher weight to the globally determined revised *Hipparcos* value would increase the derived brightness of the star by $\leqslant 0.2$ mag. We then obtain the following absolute magnitudes after adding a Lutz–Kelker (LK) correction of −0.02 which was calculated on the same basis as that adopted by Benedict et al.:

$$M_V = +0.54,\ M_{K_s} = -0.64,$$

each with standard error of ±0.11. In deriving the above figures, we have adopted the data for RR Lyrae in Table 1. The reddening, $E(B-V) = 0.030$, given there agrees with the value derived directly from its parallax distance and the Drimmel, Cabrera-Lavers & López-Corredoira (2003) formulation discussed below (0.031).

There are 142 stars, including RR Lyrae itself, in Table 1. Reduced parallax solutions (see, e.g. Feast 2002) were carried out for this group of stars. The reddenings were estimated for each star using the Drimmel et al. (2003) three-dimensional Galactic extinction model, including the rescaling factors that correct the dust column density to account for small-scale structure seen in the DIRBE data but not described explicitly by the model. Two initial estimates were made of the distance of a star using the tabulated mean K_s or V magnitudes and preliminary PL(K_s) or M_V–[Fe/H] relations, both of which correspond to an LMC modulus of ∼18.5. The results were iterated (see e.g. Whitelock, Feast & van Leeuwen 2008). The values of $E(B-V)$ tabulated and used are the means of the final results from K_s and V.

A reduced parallax solution of equation (1) for the 142 stars and adopting $a = 0.214$ then leads to

$$M_V = +0.54,$$

at the mean metallicity of the sample ($\overline{\mathrm{[Fe/H]}} = -1.38$). Similarly, reduced parallax solutions lead to

$$M_{K_s} = -0.63$$

at the mean $\log P$ of the sample ($\overline{\log P} = -0.252$), adopting a PL($K_s$) slope of −2.41 as in equation (4). The standard error of these derived absolute magnitudes is ±0.10. (Note that no LK correction is required in this case). These results are essentially identical to those for RR Lyrae itself and indeed the solution is completely dominated by this one star. Omitting RR Lyrae leads to solutions with very large standard errors. In the following, we simply use the results based on RR Lyrae alone, but using the full set of stars would obviously make no difference.

We then find

$$b = 19.39 - \mathrm{Mod(LMC)} = +0.84 \pm 0.11$$

for equation (1) with $a = 0.214$ as in equation (2). This gives absolute magnitudes brighter by 0.16 ± 0.12 than those given by equation (2) with an LMC modulus of 18.39 ± 0.05. The standard error does not take into account the scatter about the M_V–[Fe/H] relation, which can be substantial (see e.g. Gratton et al., fig. 19.). This result is consistent with the prediction of Catelan & Cortés (2008) that RR Lyrae is overluminous for its metallicity by 0.06 ± 0.01 mag compared with the average members of this class. Note that if we adopted their preferred reddening for RR Lyrae we would reduce the overluminosity implied by our result from 0.16 ± 0.12 to 0.12 ± 0.12.

Main-sequence fitting procedures (Gratton et al. 2003) lead to $b = +0.89 \pm 0.07$. However, other work (e.g. Salaris et al. 2007) has suggested a smaller distance modulus for 47 Tuc, a cluster on which the result of Gratton et al. partly depends. Thus, their value of b may need increasing slightly. The statistical parallaxes from Popowski & Gould (1998) lead to a value of $b = +1.10 \pm 0.12$, that is to absolute magnitudes 0.10 ± 0.12 fainter than equation (2).

The parallax data on RR Lyrae lead to a constant term in equation (3) of -1.12. This is 0.07 mag brighter than the value given by Sollima et al. which was based on the *HST* parallax of RR Lyrae alone and a slightly different K_s magnitude. Following the discussion in Sollima et al. (2006), which takes into account metallicities of the LMC variables, the parallax result leads to a distance modulus of the LMC which is 0.22 ± 0.14 larger than that deduced from the classical Cepheids (18.39 ± 0.05). A main uncertainty in the Cepheid result was in the metallicity correction adopted, and the RR Lyrae parallax result may indicate that this was overestimated. However, the errors are such that within the uncertainties the classical Cepheids and RR Lyrae variable scales are substantially in agreement.

4 THE TYPE II CEPHEIDS

4.1 Trigonometrical parallaxes

The relevant data for the two CephIIs on our programme are collected in Table 2. The metallicity of VY Pyx is from Maas et al. (2007). The value quoted for κ Pav is from Luck & Bond (1989). Both stars are comparatively metal-rich. The *BV* photometry of VY Pyx is from Sanwal & Sarma (1991), whilst J and K_s are single 2MASS values. In view of the low visual amplitude of VY Pyx ($\Delta V = 0.27$), these should be close to mean values. The magnitudes, light curve and period agree satisfactorily with the *Hipparcos* photometry (ESA 1997). For κ Pav, the intensity means B, V and I were derived from from the literature cited in Table 3, with I in the Cousins system. J and K_s for this star are from the intensity means given in Section 4.2.2 transformed to the 2MASS system using the relations derived by Carpenter (2001, as updated on the 2MASS web page). The reddenings for both stars were estimated on the Drimmel et al. (2003) model described in Section 3.2, with distances adopted from the revised *Hipparcos* parallaxes ($\pi \pm \sigma_\pi$) which are also listed. The distance moduli (Mod) and their uncertainties come directly from the parallaxes. The LK corrections needed in deriving the absolute magnitudes are calculated on the same system as used for RR Lyrae (Section 3). In discussing the various absolute magnitudes listed, we will use for their standard errors the values derived for the distance moduli. It should be borne in mind that these may be slightly underestimated due to any uncertainty in photometry, reddening and LK correction.

Table 2. Data for CephIIs: *Hipparcos* parallaxes.

	VY Pyx	κ Pav
$\log P$	0.093	0.959
[Fe/H]	−0.44	0.0
B	7.85	4.98
V	7.30	4.35
I		3.67
J	6.00	3.17
K_s	5.65	2.78
$E(B-V)$	0.049	0.017
π	5.00	6.51
σ_π	0.44	0.77
Mod	6.59	5.93
σ_{Mod}	0.19	0.26
LK	−0.06	−0.12
M_B	+1.09	−1.14
M_V	+0.54	−1.86
M_I		−2.41
M_{K_s}	−0.92	−3.27

There are other stars classified as CephIIs in the *Hipparcos* catalogue in addition to κ Pav and VY Pyx, but their σ_π/π values are relatively high and in some cases it is uncertain whether they belong to the CephII class. We have therefore not attempted to use these stars.

4.2 Pulsation parallaxes

4.2.1 The projection factor, p

The Baade–Wesselink (BW) method for radius determination has seen only limited use for CephIIs, even at optical wavelengths, and table 2 in Balog, Vinko & Kaszas (1997) suggests that such results as have been reported are somewhat inconsistent with each other.

For classical Cepheids, the reasons for using infrared (IR) photometry in determining pulsational parallaxes or BW radii have been given by Laney & Stobie (1995, henceforth LS95), and by Gieren, Fouqué & Gomez (1997), among others. This technique has not been used previously in determining radii, luminosities, etc., for CephIIs, except for a few preliminary results given by Laney (1975). Whilst modern pulsational parallaxes are often of high internal consistency, it has been difficult to estimate possible systematic uncertainties. Significant progress in dealing with such systematic uncertainties has become possible since the advent of reasonably accurate parallaxes for nearby classical Cepheids (Benedict et al. 2002b, 2007; van Leeuwen et al. 2007), as these allow a particular pulsational parallax method to be calibrated empirically.

Several recent papers (Merand et al. 2005; Fouqué et al. 2007; Groenewegen 2007; Nardetto et al. 2007) have tackled the determination of the projection factor (p-factor), which has long been one of the principal sources of uncertainty in pulsational parallaxes. Other papers have discussed angular diameter measurements and the surface brightness–colour relation, but these are not as directly relevant to the method used here as the radii derived in this paper have been calculated using the technique described in Balona (1977), where the surface brightness coefficient is a free parameter. Conversion

Table 3. Pulsation parallax solutions for classical Cepheids and κ Pav.

Star	Period	$\langle K_o \rangle$	$\langle J_o \rangle$	$\langle V_o \rangle$	R_1	R_2	M_K	π_1	π_2	p	Optical photometry reference	Radial velocity reference
δ Cep	5.366 2475	2.295	2.678	3.667	41.3 ± 1.0	42.5 ± 1.0	−4.86	3.71 ± .12	3.72 ± .09	1.27 ± .05	1, 2, 3	A, B, C
X Sgr	7.012 675	2.453	2.833	3.819	49.3 ± 1.6	47.3 ± 1.4	−5.16	3.17 ± .14	3.01 ± .09	1.20 ± .06	1, 4, 5, 6	D–N
β Dor	9.842 578	1.947	2.405	3.616	62.1 ± 1.7	63.0 ± 1.0	−5.64	3.26 ± .14	3.04 ± .07	1.18 ± .06	7–10	O, P
ζ Gem	10.149 92	2.128	2.605	3.884	62.7 ± 1.7	65.4 ± 1.6	−5.67	2.74 ± .12	2.76 ± .07	1.28 ± .06	1, 3, 13	A, C, Q
l Car	35.543 27	1.046	1.639	3.225	162.3 ± 4.0	165.7 ± 3.0	−7.59	2.03 ± .16	1.87 ± .04	1.17 ± .10	7, 9–11	M, R
κ Pav	9.0880	2.795	3.201	4.291	26.5 ± 0.8	26.3 ± 0.6	−3.81	6.51 ± .77	4.78 ± .13	0.93 ± .11	7, 9, 13, 15, 16	P

The columns contain: column (1) – star name, column (2) – period in days, columns (3)–(5) – intensity mean magnitudes corrected for reddening ($\langle K_o \rangle$, $\langle J_o \rangle$ in the SAAO system), columns (6) and (7) – radii in solar units derived from $K, J-K$ (R_1) and $K, V-K$ (R_2) with $p = 1.27$, column (8) – derived absolute magnitude, column (9) – the trigonometrical parallax and its standard error, column (10) – pulsational parallax and its (internal) standard error, column (11) – the projection factor p, column (12) – optical photometry references and column (13) – radial velocity references.
The errors of the mean radius and the trigonometrical parallax have been added in quadrature for σ_p.
Optical photometry references. (1): Moffett & Barnes (1984), (2): Barnes et al. (1997), (3): Kiss (1998), (4): Shobbrook (1992), (5): Arellano Ferro et al. (1998), (6): Berdnikov & Turner (2001), (7): Dean (1977), (8): Pel (1976), (9): Dean (1981), (10): Shobbrook (1992), (11): Bersier (2002), (12): Szabados (1981), (13): Dean (1977), (14): Berdnikov (1997), (15): ESA (1997), (16): Cousins & Lagerweij (1971).
Radial velocity references. (A): Bersier et al. (1994), (B): Butler (1993), (C): Kiss (1998), (D): Moore (1909), (E): Duncan (1932), (F): Stibbs (1955), (G): Feast (1967), (H): Lloyd Evans (1968), (I): Lloyd Evans (1980), (J): Barnes, Moffett & Slovak (1987), (K): Wilson et al. (1989), (L): Sasselov & Lester (1990), (M): Bersier (2002), (N): Mathias et al. (2006), (O): Taylor & Booth (1998), (P): Wallerstein et al. (1992), (Q): Gorynya et al. (1998), (R): Taylor et al. (1997).

from radii to luminosities uses a methodology described below, and is in effect included in the calibration of the p-factor.

As in LS95, solutions have been derived with a modified version of Luis Balona's software which allows for a non-negligible amplitude, and where photometric magnitudes and colours, as well as radial velocities, are assigned individual errors. All radii used were derived using K as the magnitude and $V-K$ or $J-K$ as the colour, as this approach was shown to be free of serious phase-dependent systematic error by LS95. These authors also show that inclusion or exclusion of the rising branch has a negligible systematic effect on the derived radii, although excluding the rising branch increases the uncertainty in the results. Here, J and K are on the SAAO system (see Appendix A). Adopted radii are the means of the (K, $V-K$) and (K, $J-K$) values. The adopted formal error in the radius is derived by taking the square root of the mean of the squares of the individual errors in the (K, $V-K$) and (K, $J-K$) radii.

The first necessary step is to derive an appropriate value of the p-factor *for the specific method used here*. Our radius-determination methodology is different from those used by Merand et al. (2005), Groenewegen (2007) and Nardetto et al. (2007), and the radial velocities (selected from the literature) are not based on a single selected line, as described by Nardetto et al. (2007).

As a first approximation, $p = 1.27$ (Merand et al. 2005; Groenewegen 2007) was adopted, and radii were calculated for five of the classical Cepheids in table 2 of van Leeuwen et al. (2007). Polaris has a limited, variable amplitude and we are unaware of suitable data for an accurate radius solution. For FF Aql, the possible influence of a binary companion and the low quality of the *JHK* data were enough to drop it from the list. The other stars in the van Leeuwen et al. list have higher σ_π/π than our five stars.

For the remaining five stars, the ($K, V-K$) and ($K, J-K$) radii were calculated with $p = 1.27$, and then converted into luminosities. This was done using the tables given in Hindsley & Bell (1990) to establish the K-band absolute magnitudes for a star of one solar radius and the appropriate dereddened $V-K$ and $J-K$ colours, and then taking the mean. As discussed in LS95, the K surface brightness as a function of $J-K$ or $V-K$ is very insensitive to surface gravity or microturbulence, which means that neither the radius solution nor the derived luminosity is significantly affected by assumptions about mean or time-varying values for these quantities in the stellar atmosphere. A similar procedure was followed for κ Pav, the only CephII which has good *JHK* and radial velocity data and a usable parallax measurement – though this is of lower quality than for the five classical Cepheids. Dereddening was done using the reddening coefficients derived by Laney & Stobie (1993), and BVI_C reddenings for each star as calibrated recently by Laney & Caldwell (2007), using metal abundances from the tables in that paper, or for κ Pav the value from Luck & Bond (1989). The resulting small uncertainty in the colours has only a small effect on the K surface brightness, as it is only a weak function of either $V-K$ or $J-K$. Figs 1–6 show the match of radius displacements calculated from the radius solution and *VJK* photometry to the integrated radial velocity curve. As would be expected from LS95, there are no serious phase anomalies or discrepancies. Any serious problems with shock waves, etc., that distorted the solutions should appear in these diagrams, but there is no real sign of such an effect – even for X Sgr (Sasselov & Lester 1990; Mathias et al. 2006) or κ Pav. For any other value of the projection factor, the curves would appear identical to those shown except that the vertical scale would be slightly different.

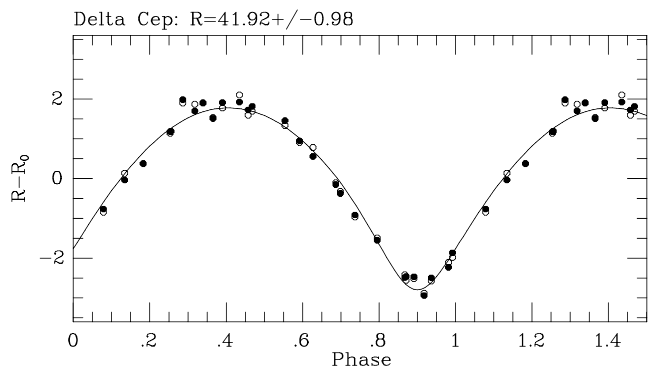

Figure 1. Radius displacements for δ Cep calculated from the $K, J-K$ (open circles) and $K, V-K$ (filled circles) radius solutions and photometry, versus the integrated radial velocity curve (solid line). A projection factor of $p = 1.27$ was used.

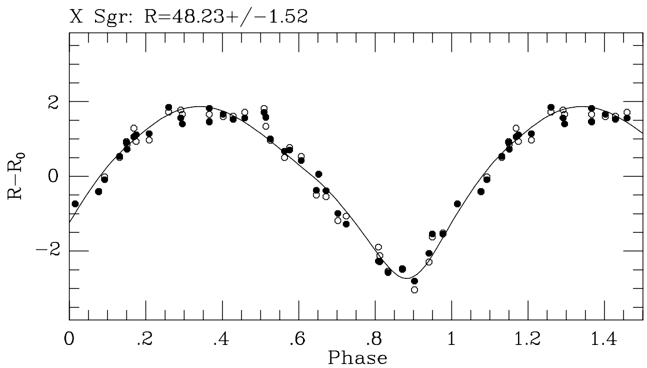

Figure 2. The same as Fig. 1, but for X Sgr.

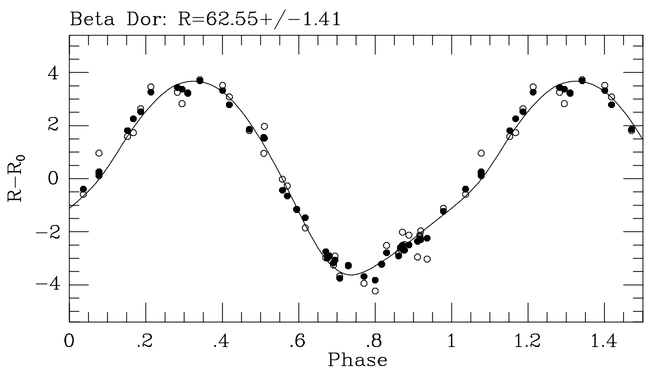

Figure 3. The same as Fig. 1, but for β Dor.

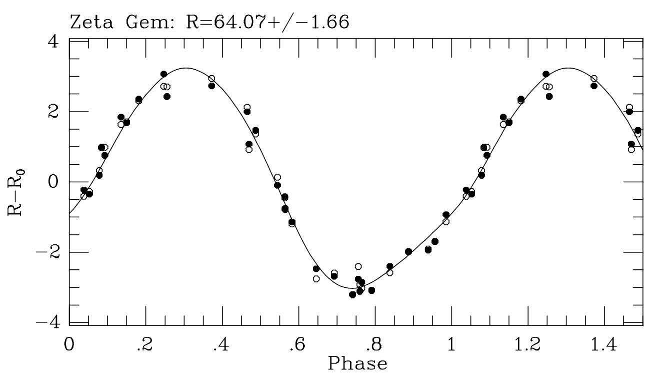

Figure 4. The same as Fig. 1, but for ζ Gem.

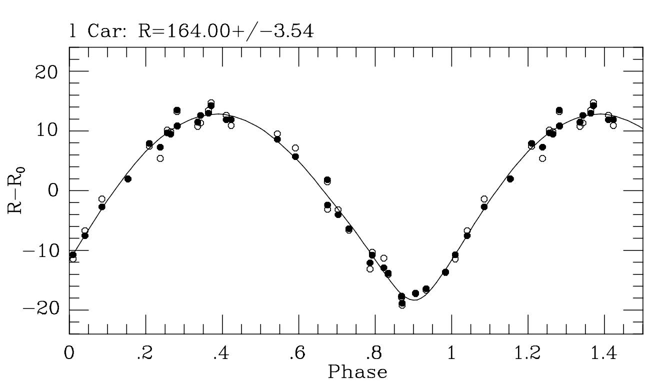

Figure 5. The same as Fig. 1, but for *l* Car.

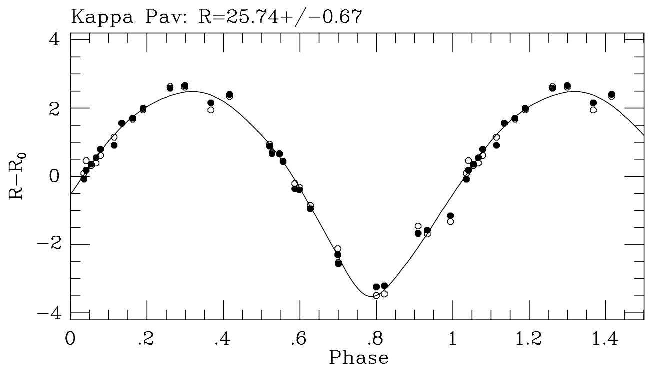

Figure 6. The same as Fig. 1, but for κ Pav.

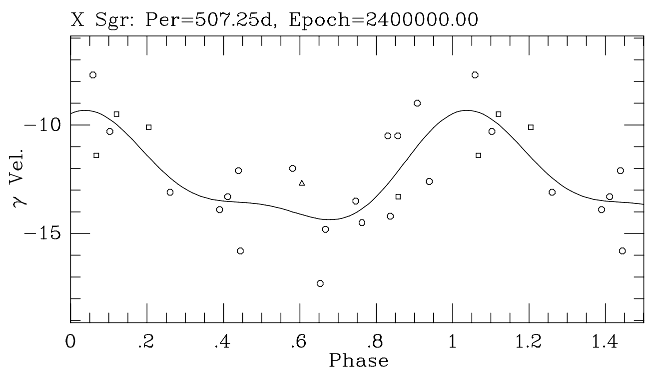

Figure 7. γ velocities for X Sgr, phased according to the ephemeris and period of Szabados (1990). The squares represent data from Bersier (2002) and Sasselov & Lester (1990). The triangle is the value from Mathias et al. (2006).

In all cases, it was necessary to establish the phase and period behaviour of the star, so that there were no systematic shifts between the phases or zero-points of the optical photometry, IR photometry and radial velocities. For X Sgr, it was also necessary to re-determine the orbital velocity curve, in view of the doubts expressed by Mathias et al. (2006). All velocities in the literature for this star, including the most recent, appear to be consistent with the orbital period determined by Szabados (1990), and it proved possible to separate the orbital and pulsational velocities effectively (Fig. 7), though better data are desirable. The *JHK* data used are listed in Appendix A.

Radii, luminosities and pulsational parallaxes for the five classical Cepheids and κ Pav, derived as above for $p = 1.27$, are given in Table 3, together with the sources for the optical photometry and radial velocities. Also in this table are the trigonometrical parallaxes from van Leeuwen et al. (2007) and this paper. Requiring that the *p*-factor for each star be adjusted to produce agreement between the pulsation and trigonometrical parallaxes leads to the empirical *p*-factors for each star listed in Table 3 together with the associated errors due to the uncertainties in both the radius and the trigonometrical parallax. These lead to the empirical *p*-factor for each star listed in the table together with the associated errors due to uncertainty in the radius and in the parallax. These values of *p* are plotted against $\log P$ in Fig. 8. For all five classical Cepheids, the derived *p*-factor falls within a narrow range, and the mean is 1.22 ± 0.02, weighting the stars equally. An average, weighted according to the inverse square of the error, gives 1.23 ± 0.03 where the weight of *l* Car has been set to 1 and its error has been divided by the square root of the sum of the weights for all five stars . A trend with period

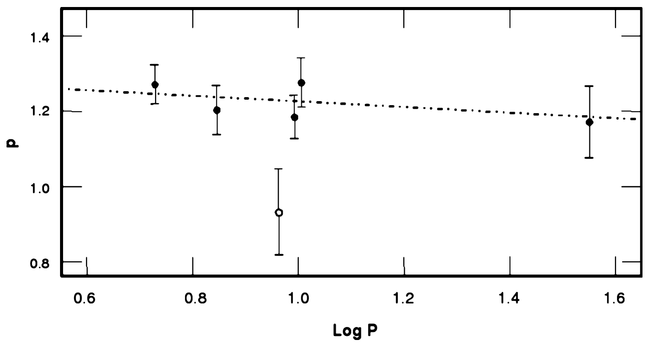

Figure 8. The projection factor, p, plotted against $\log P$ for the classical Cepheids, δ Cep, X Sgr, β Dor, ζ Gem and l Car (filled circles) and the CephII κ Pav (open circle). The line shows the trend of p with period suggested by Nardetto et al. (2007), but adjusted to the zero-point given by the five classical Cepheids.

may be present, as claimed in Nardetto et al. (2007), though our sample is too small to derive a useful, statistically significant value of a term in $\log P$. If we assume that there is a $\log P$ term of -0.075 (given by Nardetto et al. as appropriate for velocities based on a mix of lines of varying depth), the weighted intercept at $\log P = 1.0$ is 1.23 ± 0.03.

The derived p-factor for κ Pav, on the other hand, is strikingly discrepant, so low as to be physically unrealistic, especially given that the colours and surface gravity are in reasonable accord with those given for classical Cepheids by Laney & Stobie (1995) and Fernie (1995) respectively, while the metallicity is solar (Luck & Bond 1989) and the radius displacement diagram (Fig. 6) resembles those of the five classical Cepheids. However, the parallax for this star is more uncertain than for the five classical Cepheids, and the derived p-factor is in fact only about 2σ from the weighted mean of the five classical Cepheids. A p-factor of 1.23 was adopted for all three CephIIs considered here.[4] Details of the radius and luminosity determinations follow. Magnitudes, radii, absolute magnitudes and other relevant data are given in Tables 4 and 5.

4.2.2 κ Pav

The best-fitting period for the IR data in Table A1 [Julian Date (JD) 244 5928–244 7769] was 9.0814 d, and the scatter around a low-order (2–5) Fourier fit to the resulting magnitudes and colours was about 0.009–0.011 mag. This is rather higher than normal for such a bright star, and suggests a modest amount of phase jitter may have been present.

Contemporaneous radial velocity data were available in the literature (Wallerstein et al. 1992), covering almost exactly the same range of JDs. A modest number of velocities with slightly later JD were shifted into phase agreement at the adopted period. The light curve of κ Pav is known for sudden changes (Wallerstein et al. 1992), so a need for phase adjustments is not surprising.

The sources of the visual photometry are given in Table 3. All data sets have been phased at their appropriate periods, and then shifted into phase and zero-point agreement with Dean (1977) and Dean (1981). This composite data set was used to derive a sixth-order Fourier fit to the V light curve, with maximum light in V set to phase 0. None of the optical photometry data sets was contemporary with the IR data. Derived periods and epochs were

244 0140.119 + 9.0947E (Cousins & Lagerweij),
244 1959.499 03 + 9.083 52E (Dean et al., Dean).
244 8164.8647 + 9.092 405E (Shobbrook, *Hipparcos*, Berdnikov, Berdnikov & Turner).

A V magnitude was then calculated for each IR observation, using an epoch for the IR data which ensured that a Fourier fit to the $V-K$ and $J-K$ data gave phases for minimum light in agreement with those for $B-V$ and $V-I$, a technique for phase alignment validated by LS95. The resulting $(K, J-K)$ and $(K, V-K)$ radii agree within less than 1 per cent, and there are no significant phase-dependent anomalies (Fig. 6).

$E(B-V) = 0.017 \pm 0.022$ was derived from the $B-V$ and $V-I$ magnitude means (and the solar metallicity given by Luck & Bond 1989), using the Cousins reddening method as re-calibrated by Laney & Caldwell (2007). While this method has not been specifically calibrated for CephIIs, κ Pav falls into much the same range in temperature, surface gravity and metallicity as classical Cepheids. This reddening is virtually the same as that derived by the Drimmel method (0.019). The reddening value is in any event not critical – it affects the luminosity and distance determinations *only* through the weak dependence of K surface brightness on the dereddened $V-K$ and $J-K$ colour indices.

Dereddened $V-K$ and $J-K$ colours were used to calculate the surface brightness at K as described above, using $\log g$ of 1.2 (Luck & Bond 1989), and converted to absolute magnitudes at V, J and K using the mean radius and the dereddened empirical colours. 2MASS J, H and K_s, absolute magnitudes were calculated using the transformations on the 2MASS website, as they also were for V553 Cen and SW Tau, below.

4.2.3 V553 Cen

The period behaviour is simpler than for κ Pav, and seems to be adequately described by

244 8437.1154 + 2.060 464E(244 4423–245 0364),
244 3108.6572 + 2.060 608E(244 0700–244 3686).

These phases were adopted for the IR photometry (Table A1), for optical photometry by Wisse & Wisse (1970), Lloyd Evans, Wisse & Wisse (1972), Dean (1977, 1981), Eggen (1985), Diethelm (1986), Gray & Olsen (1991), ESA (1997), Berdnikov & Turner (1995) and Berdnikov (1997), and for radial velocities by Wallerstein & Gonzalez (1996) and Lloyd Evans et al. (1972). All optical photometry was adjusted in zero-point to match Dean (1977) and Dean (1981), and the radial velocities to match Wallerstein & Gonzalez.

The mean $E(B-V)$ for solar metallicity and a microturbulence of 2.5 km s^{-1} (Wallerstein & Gonzalez 1996) is 0.00 ± 0.02 from 54 observations with $B-V$ and $V-I$. These authors also derive $\log g \sim 1.8$. The Drimmel procedure gives $E(B-V) = 0.08$.

The derived $(K, J-K)$ and $(K, J-K)$ radii agree within the errors, and the lack of significant phase-dependent anomalies can be seen in Fig. 9.

4.2.4 SW Tau

The period seems essentially constant at 1.583 565 d over the relevant interval, with an epoch of 244 5013.2696 for maximum light in V. Optical photometry has been taken from Barnes et al. (1997), Moffett & Barnes (1984) and Stobie & Balona (1979), and the zero-point shifted to match Stobie & Balona. For $B-V$ and $V-I$

[4] See also the discussion in Section 5.1.

Table 4. Pulsation parallax results for CephIIs.

Star	Period	$\langle K_o \rangle$	$\langle H_o \rangle$	$\langle J_o \rangle$	$\langle V_o \rangle$	R_1	R_2	D
SW Tau	1.583 565	7.887	7.931	8.147	8.800	8.02 ± 0.27	8.03 ± 0.15	$732 \pm 20 \pm 16$
V553 Cen	2.060 464	6.878	6.963	7.290	8.455	10.53 ± 0.33	10.20 ± 0.25	$541 \pm 15 \pm 12$
κ Pav	9.0902	2.795	2.863	3.201	4.291	26.48 ± 0.78	26.32 ± 0.62	$204 \pm 5 \pm 4$

The columns are: column (1) – star name, column (2) – period in days (for κ Pav this is the mean of the three periods used for the optical photometry), columns (3)–(6) – intensity mean magnitudes with the IR values on the SAAO system, columns (7) and (8) – radii in solar units from, $K, J-K$ (R_1) and $K, V-K$ (R_2), column (9) – distance in pc based on a mean of R_1 and R_2 and with $p = 1.23$ (the first standard error reflects the uncertainty in the derived radius, and the second standard error reflects the uncertainty in p).

Table 5. Data for CephIIs: pulsational parallaxes.

	κ Pav	V553 Cen	SW Tau
$\log P$	0.959	0.314	0.200
[Fe/H]	0.0	+0.24	+0.22
B	4.98	9.15	10.32
V	4.35	8.46	9.66
I	3.67	7.76	8.94
K_s	2.78	6.86	7.95
K_W	2.55	6.63	7.73
$E(B-V)$	0.017	0.00	0.282
Mod	6.55	8.67	9.32
σ_{Mod}	0.07	0.08	0.08
M_B	−1.64	+0.48	−0.15
M_V	−2.25	−0.21	−0.53
M_I	−2.91	−0.90	−0.88
M_{K_s}	−3.77	−1.80	−1.46

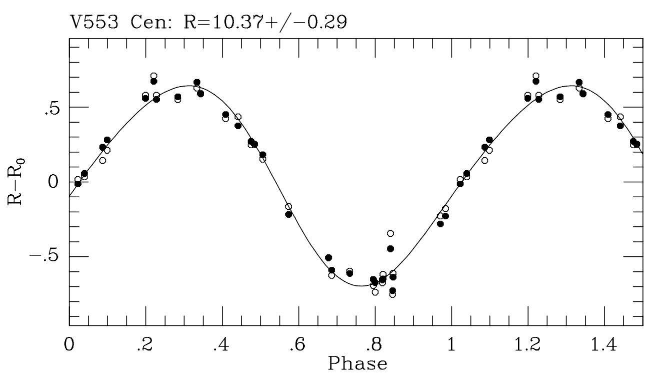

Figure 9. The same as Fig. 1, but for V553 Cen and adopting $p = 1.23$.

magnitude means of 0.653 and 0.796 on the Cousins system, with [Fe/H] = +0.2, and microturbulence of 3.0 km s^{-1} (Maas et al. 2007), $E(B-V)$ is 0.282 ± 0.031. $\log g$ from Maas et al. is about 2.0. The Drimmel procedure gives $E(B-V) = 0.26$.

IR data for SW Tau on the CIT system were taken from Barnes et al. (1997) and transformed to the Carter system by the formulae given in Laney & Stobie (1993). This was then combined with the SAAO *JHK* observations, and matched to the SAAO zero-point. As would be expected, the resulting shifts were small.

Radial velocities used are those from Gorynya et al. (1998) and from Bersier et al. (1994).

The derived $(K, J-K)$ and $(K, J-K)$ radii agree within the errors, and the lack of significant phase-dependent anomalies can be seen in Fig. 10.

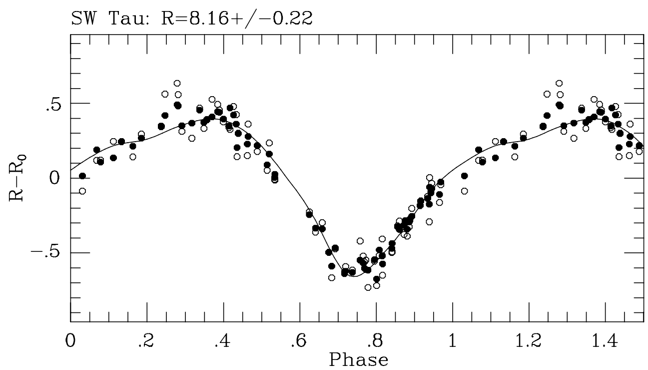

Figure 10. The same as Fig. 1, but for SW Tau and adopting $p = 1.23$.

5 DISCUSSION

5.1 κ Pav

The trigonometrical and pulsational parallaxes of κ Pav are 6.51 ± 0.77 and 4.90 ± 0.17, a difference of 1.61 ± 0.79. This 2σ difference is sufficiently large to raise some concerns. The *Hipparcos* result is from a type 3 solution. In such a solution, account is taken of possible variability induced motion. Further investigation shows evidence (Fig. 11) for a magnitude dependence difference between the DC and AC *Hipparcos* magnitudes. These magnitude systems and the interpretation of differences between them are described in the *Hipparcos* catalogue (ESA 1997). The results for κ Pav suggest the presence of a close companion consistent with the need for a type 3 solution. Given the method of reduction employed, the revised *Hipparcos* parallax should be reliable within the quoted uncertainty.

The possibility that κ Pav was a spectroscopic binary was suggested by Wallerstein et al. (1992) from a comparison of their work with much earlier observations. There is, however, no evidence of short-period variations in γ velocity in their data which extended over a considerable time span (JD 244 5860–244 8283) or the additional data we have used. The five-colour photometry of Janot-Pacheco (1976) shows no evidence of a bright companion. This work provides internal checks on the possibility of a bright companion. A bright red companion would produce abnormally low surface brightness coefficients in the $(K, J-K)$ and, especially, the $(K, V-K)$ solutions. A companion of similar colour to the variable would affect the two solutions more equally. In fact, these two surface brightness coefficients are slightly higher for κ Pav than the other two CephIIs in the programme, though not significantly so. A blue companion would tend to make the $(K, V-K)$ radius smaller than the $(K, J-K)$ one. The $(V, B-V)$ radius would be smaller still and have an unusually large surface brightness coefficient as

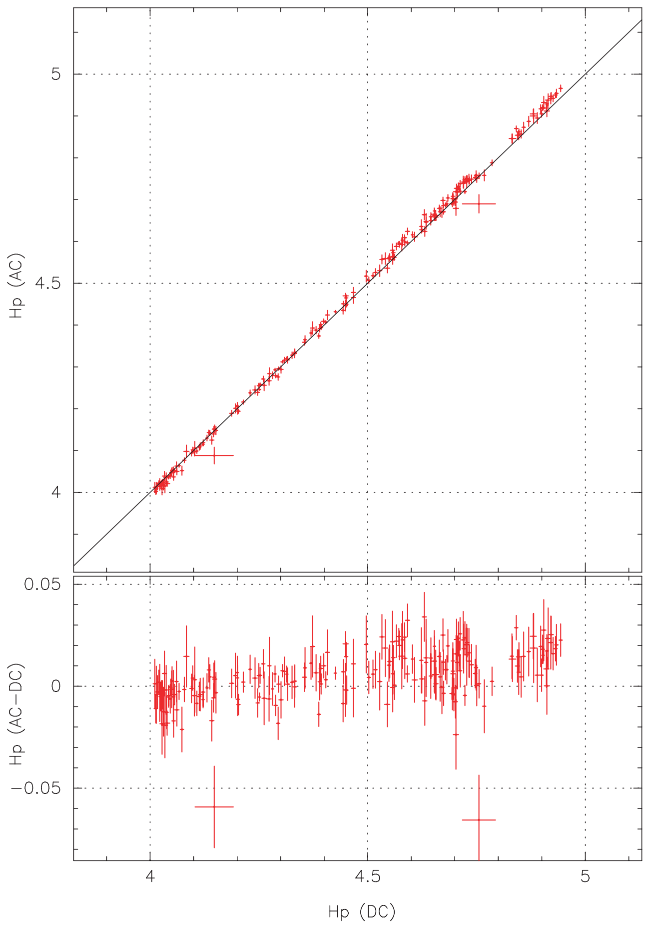

Figure 11. The relation between the *Hipparcos* AC and DC magnitudes for κ Pav. The increasing discrepancy between the AC and DC magnitudes towards fainter magnitudes is an indication for the presence of a close companion that becomes more visible as κ Pav becomes fainter.

seen in the classical Cepheid binary KN Cen (LS95). In κ Pav, there is no significant difference between the $(K, V-K)$ and $(K, J-K)$ radii. The $(V, B-V)$ radius is smaller by 13 per cent. This is a marginal effect and indicates that any blue companion has a relative brightness considerably fainter than in the case of KN Cen.

Thus, in summary, no serious anomalies were found in the pulsational parallax analysis besides the problem of phase shifts. However, some caution is necessary in discussing this star. In the following, we discuss the results separately for the two estimates of the parallax.

5.2 Infrared period–luminosity relations

Table 6 lists the differences of the parallax based absolute magnitudes from the PL(K_s) relation (equation 4). We adopt $c = -1.0$ corresponding to an LMC modulus of 18.39. Besides the CephII stars, Table 6 lists, in addition, the results for RR Lyrae. As already noted, Matsunaga et al. (2006) suggested that the RR Lyrae variables lay on the same PL(K_s) relation as the CephIIs and this suggestion was strengthened by the work of Sollima et al. (2006). Two standard errors are given: σ_1 is the value derived from the parallax solution and σ_2 combines this in quadrature with the scatter in the PL(K_s) relation as given by Matsunaga et al. (2006) (0.14). The latter value is an upper limit to the intrinsic scatter of the Matsunaga et al. relation since it includes uncertainties in the moduli of the globular clusters they used, etc. The first part of Table 6 shows the results from the trigonometrical parallaxes and the second part shows the results from the pulsational parallaxes.

Table 6. Differences from IR PL relations.

Star	ΔM_K	σ_1	σ_2
	(a)		
RR Lyrae	−0.24	0.11	0.17
VY Pyx	+0.30	0.19	0.24
κ Pav	+0.04	0.26	0.30
	(b)		
κ Pav	−0.46	0.07	0.16
V533 Cen	−0.05	0.08	0.16
SW Tau	+0.02	0.08	0.16

(a): Results using trigonometrical parallaxes.
(b): Results using pulsational parallaxes.

Given the uncertainties in the trigonometrical parallaxes, the results in the first part of Table 6 show satisfactory agreement with the predictions of the IR PL relation. The two short-period stars with pulsational parallaxes (SW Tau, $P = 1.58$; V553 Cen, $P = 2.06$) agree closely with predictions. This agreement is sufficiently good to hint that the intrinsic scatter in the relations is less than the adopted 0.14, in agreement with the discussion above. Indeed, if the possible period dependence of the projection factor p discussed in Section 4.2.1 applies, these two stars lie even more closely on a line with the Matsunaga et al. slope. They would then be 0.09 mag (V553 Cen) and 0.08 mag (SW Tau) brighter than that predicted using a zero-point based on an LMC modulus of 18.39. Both SW Tau and V553 Cen are carbon-rich stars of near-solar metallicity. SW Tau has [Fe/H] = +0.22 (Maas et al. 2007) and V553 Cen has [Fe/H] = +0.04 (Wallerstein & Gonzalez 1996). The light curve classification scheme proposed by Diethelm (1990 and other papers referenced there) indicates that, as one would expect, these two stars are disc objects. On the other hand, the short-period globular cluster stars ($P < 5$ d) in Matsunaga et al. (2006) are all of low metallicity ([Fe/H] in the range −1.15 to −1.94). Thus, within the uncertainties, the PL(K_s) relation for CephIIs is insensitive to population differences (metallicity, mass) at least at the short-period end.

The pulsational parallax of κ Pav leads to an IR absolute magnitude that differs significantly from the PL relations derived from the globular clusters and with an LMC modulus of 18.39. Since the formal uncertainty of the pulsation-based absolute magnitude is 0.07 mag, the deviation is 6.5σ and even taking into account the upper limit on the intrinsic scatter in the PL(K_s) relation there is nearly a 3σ deviation. Evidently, if this result is accepted then some CephIIs in the field can deviate significantly from the PL(K_s) based on globular cluster variables. Since the metallicity of κ Pav is near-solar and the results of Matsunaga et al. depend on metal-poor objects, a (large) metallicity effect might be the cause. As there is little metallicity dependence among the metal-poor objects (see Section 2.2), this would imply a very non-linear dependence on metallicity. An age/mass difference would be another possible cause (possibly operating more strongly among the longer period CephIIs like κ Pav than among the shorter period one).

If one adopts the results from the three pulsational parallaxes, an LMC modulus of 18.55 ± 0.15 is implied, neglecting any metallicity effect on CephII luminosities. This agrees with the RR Lyrae result given above which implies a modulus of 18.55 ± 0.12. Neither of these values are significantly different from the classical

Cepheid result (18.39 ± 0.05). However, the smaller distance for κ Pav indicated by the revised *Hipparcos* result and the discussion of Section 5.1, suggests that, for the present, the results for this star should be viewed with some caution. Additional pulsational parallaxes of CephIIs with periods near 10 d and/or an improved trigonometrical parallax of κ Pav would no doubt throw more light on this problem.

5.3 A type II Cepheid distance scale

In Section 5.2, we compared the Galactic CephII distance scale with that implied by the classical Cepheid scale (with metallicity corrections). In this section, we derive distance moduli for the LMC and for the Galactic Centre, based directly on CephIIs. The two stars V553 Cen and SW Tau give a mean zero-point, c in equation (4) of -1.01 ± 0.06, where the standard error comes from the standard errors of the two stars. If the pulsational parallax result for κ Pav is included, the zero-point becomes $c = -1.16 \pm 0.15$, where the standard error is based on the interagreement of the three stars.

Matsunaga et al. (2006) list 2MASS, single-epoch, J, H and K_s photometry of LMC CephII stars with known periods from Alcock et al. (1998). There are 21 such stars with $\log P < 1.50$. Longer period stars are not considered here as they may be RV Tau stars. After correcting by $A_{K_s} = 0.02$ mag for absorption, these data were fitted to a line of the slope derived by Matsunaga et al. equation (4) viz:

$$K_s^o = -2.41 \log P + \gamma. \qquad (8)$$

We then find $\gamma = 17.31 \pm 0.08$ or if one somewhat discrepant star is omitted $\gamma = 17.36 \pm 0.07$. With the values of c in the previous paragraph, these lead to the following estimates of the LMC modulus: for 21 LMC stars, a modulus of 18.31 ± 0.10 from V553 Cen and SW Tau, or 18.47 ± 0.17 if we included κ Pav. Leaving out the discrepant LMC star, we obtain for the two or three star solutions, 18.37 ± 0.09 and 18.52 ± 0.16. Pending further work on κ Pav, the best value is probably 18.37 ± 0.09 but none of the values deviate significantly from the classical Cepheid value 18.39 ± 0.05.

Groenewegen, Udalski & Bono (2008) have recently estimated mean K_s values and periods for 39 CephIIs in the Galactic bulge. After correction for absorption, they fitted their data to an equation equivalent to equation (8) above. Their result gives $\gamma = 13.404 \pm 0.013$. This together with the results for V553 Cen and SW Tau leads to a modulus of the Galactic Centre of 14.42 ± 0.06 and to a Galactic Centre distance of $R_0 = 7.64 \pm 0.21$ kpc. If we include κ Pav we obtain 14.56 ± 0.15 and $R_0 = 8.18 \pm 0.56$ kpc. The first value, which at present should probably be considered the preferred one, is close to that obtained by Eisenhauer et al. (2005) from the motion of a star close to the central black hole. With the suggested relativistic correction of Zucker et al. (2006), this is $R_0 = 7.73 \pm 0.32$ kpc. The value with κ Pav included does not differ significantly from the latter result.

5.4 Optical period–luminosity relations

The relations derived for CephIIs in the globular clusters NGC 6441 and NGC 6388 (equations 5–7 above) at optical wavelengths, are quite narrow (see Pritzl et al. 2003, fig. 8). On the other hand, plots of PL diagrams in B, V or I for all known data for globular clusters and the LMC (e.g. Pritzl et al., fig. 9) show very considerable scatter. Pritzl et al. suggested that at least part of this scatter might be due to poor photometry. This left open the question as to whether general PL relations are as narrow as they found for their two clusters. In Table 7 are the deviations of our programme stars from equations (5)–(7). The first part of Table 7 gives the results from the trigonometrical parallaxes and the second part of Table 7 gives those from the pulsational parallaxes. In the case of the trigonometrical result for κ Pav, the deviations are within the expected uncertainty (0.26) whereas they are large for the pulsational parallax result which has a small internal error (0.07). As discussed in Section 5.1, we prefer to leave a solution of this matter to further work. The pulsational parallax results for V553 Cen and SW Tau are of special interest since their formal uncertainties are small (0.08). These two stars have deviations of opposite signs both from the optical and from the IR relations (Tables 6 and 7). The difference between these two deviations thus gives an estimate of the lower limit of the PL width at different wavelengths, independent of PL zero-point considerations. These differences are: 0.77 mag at B, 0.51 at V, 0.20 at I and 0.07 at K_s. The results for VY Pyx, though of lower accuracy, agree with these results. This increase in the dispersion with decreasing wavelength is, as in the case of classical Cepheids, naturally explained by the existence of a finite instability strip.

Table 7. Deviation from optical relations.

Star	Equation (6) ΔM_B	Equation (5) ΔM_V	Equation (7) ΔM_I
		(a)	
VY Pyx	+0.89	+0.64	
κ Pav	−0.27	−0.34	−0.10
		(b)	
κ Pav	−0.77	−0.77	−0.60
V553 Cen	+0.56	+0.26	+0.09
SW Tau	−0.21	−0.25	−0.11

(a): Results using trigonometrical parallaxes.
(b): Results using pulsational parallaxes.

The optical differences just quoted are significantly greater than the rms scatter about the PL relations in NGC 6441 and NGC 6388 given by Pritzl et al. (2003) which are 0.10, 0.07 and 0.06 in B, V and I. The possibility that the greater optical differences estimated from V553 Cen and SW Tau are due to the adoption of incorrect reddening corrections for these two stars seems unlikely. The lower scatter in the case of the clusters is thus probably due to the smaller range in the masses of the cluster variables compared with the field.

The evolutionary state of the metal-rich, short-period CephIIs in the field has long constituted something of a puzzle (see, for instance, section 4 of Wallerstein 2002). As briefly summarized in Section 1, the short-period CephII stars are thought to be moving through an instability strip as they evolve from the blue HB towards the AGB. Old metal-rich globular clusters have, in general, only stubby red HB and it is not clear how stars of the ages and metallicities of these systems could evolve into the CephII instability strip. NGC 6441 and NGC 6388 are well known as metal-rich systems which do have extended blue HBs. There has been much discussion in the literature on the cause of this anomaly in these and similar clusters. One possibility is that the effect is due to enhanced helium abundance derived from earlier generations of stars in the clusters (see, for instance, Lee, Gim & Casetti-Dinescu 2007, Caloi & D'Antona 2007, based on earlier work by Rood 1973 and others). This seems unlikely to apply to field, short-period, metal-rich CephIIs. Thus, either an alternative explanation has to be found which will apply to both the field and the cluster stars, or, some other means need to be found to move the field stars into the instability strip.

6 CONCLUSIONS

Parallaxes of RR Lyrae variables from the revised *Hipparcos* catalogue (van Leeuwen 2007a) have been investigated. The parallax of RR Lyrae itself obtained by combining the revised *Hipparcos* value with an *HST* determination (Benedict et al. 2002a) outweighs that of all other members of the class. It yields $M_V = +0.54 \pm 0.11$ which is 0.16 ± 0.12 mag brighter than that implied by observations of RR Lyrae variables in the LMC with a modulus of 18.39 ± 0.05 derived from classical Cepheids (Benedict et al. 2007; van Leeuwen et al. 2007). For 142 *Hipparcos* RR Lyrae variables, mean J, H and K_s based on phased-corrected 2MASS values are given. These should be useful when discussing the proper motions and radial velocities of the stars. Revised *Hipparcos* parallaxes for the CephIIs κ Pav and VY Pyx are given, and pulsational parallaxes for κ Pav, V553 Cen and SW Tau derived. Extensive new J, H, K photometry of some of these stars and of some classical Cepheids is tabulated. The latter data are used to establish 1.23 as the most appropriate 'p-factor' to use in the pulsational analysis of Cepheids. The short-period, metal- and carbon-rich, disc population CephIIs, V553 Cen and SW Tau, have pulsation-based absolute magnitudes of high internal accuracy (± 0.08 mag). They fit closely (mean deviation 0.02 mag) the PL(K_s) relation derived by Matsunaga et al. (2006) from CephIIs in globular clusters and with a zero-point fixed by adopting an LMC modulus of 18.39. The *Hipparcos* parallax of the short-period star VY Pyx, although it has higher uncertainty, agrees with this result. This suggests that at least at short periods the CephIIs in the Galactic disc and in globular clusters fit the same PL(K_s) relation rather closely. The scatter of V553 Cen and SW Tau about the optical PL relations derived by Pritzl et al. (2003) for the globular clusters NGC 6388 and NGC 6441 is much greater than that about the Matsunaga PL(K_s) relation, showing the expected increase in PL widths with decreasing wavelength. This scatter about the optical relations is also much greater than that of the CephIIs in NGC 6388/6441 themselves. Since the values of [Fe/H] are very similar for V553 Cen and SW Tau, this is unlikely to be due to a metallicity effect. It presumably indicates a larger spread in masses for the short-period CephIIs in the general field than for those in the clusters.

The *Hipparcos* and pulsational parallaxes of the long-period star κ Pav differ by about 2σ. If the pulsational parallax is adopted, the value of M_{K_s} (which is of high internal accuracy, $\sigma = 0.07$ mag) is more than 6σ from the Matsunaga relation with a zero-point fixed by an LMC modulus of 18.39 and would suggest a significant mass or metallicity effect at about this period ($\sim$10 d). There are indications that this star may have a close companion. In view of this, further work on the star and of others of similar period is desirable before discussing in detail the implications for long-period CephIIs.

The results for V553 Cen and SW Tau together with published data on CephIIs in the LMC and the Galactic bulge lead to an LMC modulus of 18.37 ± 0.09 and to a distance to the Galactic Centre of $R_0 = 7.64 \pm 0.21$ kpc. Including the data for κ Pav would increase these estimates by $\sim$0.15 mag.

ACKNOWLEDGMENTS

This publication makes use of data products from 2MASS, which is a joint product of the University of Massachusetts and the Infrared Processing and Analysis Centre/California Institute of Technology, funded by the National Aeronautics and Space Administration and the National Science Foundation. We are grateful for the referee's comments.

REFERENCES

Alcock C. et al., 1998, AJ, 115, 1921
Arellano Ferro A., Rojo Arellano E., Gonzalez-Bedolla S., Rosenzweig P., 1998, ApJS, 117, 167
Balog Z., Vinko J., Kaszas G., 1997, AJ, 113, 1833
Balona L. A., 1977, MNRAS, 178, 231
Barnes T. G., Moffett T. J., Slovak M. H., 1987, ApJS, 65, 307
Barnes T. G., Moffett T. J., Freuh M. L., 1992, PASP, 104, 514
Barnes T. G., Fernley J. A., Frueh M. L., Navas J. G., Moffett I. J., Skillen I., 1997, PASP, 109, 645
Benedict G. F. et al., 2002a, AJ, 123, 473
Benedict G. F. et al., 2002b, AJ, 124, 1695
Benedict G. F. et al., 2007, AJ, 133, 1810
Berdnikov L. N., 1997, CDS Vizier Catalogue II/217
Berdnikov L. N., Turner D. G., 1995, PAZh, 21, 803
Berdnikov L. N., Turner D. G., 2001, ApJS, 137, 209
Bersier D., 2002, ApJS, 140, 465
Bersier D., Burki G., Mayor M., Duquennoy A., 1994, A&AS, 108, 25
Butler R. P., 1993, ApJ, 415, 323
Caloi V., D'Antona F., 2007, A&A, 463, 949
Carpenter J. M., 2001, AJ, 121, 2851
Carter B. S., 1990, MNRAS, 242, 1
Catelan M., Cortés C., 2008, ApJ, 676, L135
Cester B., Todoran I., 1976, MemSAI, 47, 217
Clementini G., Ripepi V., Bragaglia A., Martinez Fiorenzano A. F., Held E. V., Gratton R. G., 2005, MNRAS, 363, 734
Cousins A. W. J., Lagerweij H. C., 1971, Mon. Not. Astron. Soc. S. Afr., 30, 13
Cutri R., Skrutskie M., Van Dyk S., Beichmann C., Carpenter J., Chester T. et al., 2003, University of Massachusetts and Infrared Processing and Analysis Centre (IPAC/California Institute of Technology)
Elias J. H., Frogel J. A., Matthews K., Neugebauer G., 1982, AJ, 87, 1029 (Erratum 1982, AJ, 87, 1893)
Elias J. H., Frogel J. A., Hyland A. R., Jones T. J., 1983, AJ, 88, 1027
Dean J. F., 1977, Mon. Not. Astron. Soc. S. Afr., 36, 3
Dean J. F., 1981, SAAO Circ., 6, 10
Dean J. F., Cousins A. W. J., Bywater R. A., Warren P. R., 1977, Mem. R. Astron. Soc., 83, 69
Diethelm R., 1986, A&AS, 64, 261
Diethelm R., 1990, A&A, 239, 186
Drimmel R., Cabrera-Lavers A., López-Corredoira M., 2003, A&A, 409, 205
Duncan J. C., 1932, PASP, 44, 324
Eggen O. J., 1985, AJ, 90, 1297
Eisenhauer F. et al., 2005, ApJ, 628, 246
ESA, 1997, The *Hipparcos* catalogue ESA SP-1200
Feast M. W., 1967, MNRAS, 136, 141
Feast M. W., 2002, MNRAS, 337, 1035
Fernie J. D., 1995, AJ, 110, 2361
Fernley J. A., Skillen I., Jameson R. F., Longmore A. J., 1990, MNRAS, 242, 685
Fernley J. A., Skillen I., Burki G., 1993, A&AS, 97, 815
Fernley J. A., Barnes T. G., Skillen I., Hawley S. L., Evans D. W., Solano E., Garrido R., 1998, A&A, 330, 515
Fouqué P. et al., 2007, A&A, 476, 73
Gieren W. P., Fouqué P., Gomez M. I., 1997, ApJ, 488, 74
Gieren W. P., Fouqué P., Gomez M. I., 1998, ApJ, 496, 17
Gingold R. A., 1976, ApJ, 204, 116
Gingold R. A., 1985, Mem. Soc. Astron. Ital., 56, 169
Gorynya N. A., Samus N. N., Sachkov M. E., Rastorguev A. S., Glushkova E. V., Antipin S. V., 1998, Astron. Lett., 24, 815
Gratton R. G., Bragaglia A., Carretta E., Clementini G., Desidera S., Grundahl F., Lucatello S., 2003, A&A, 408, 529
Gratton R. G., Bragaglia A., Clementini G., Carretta E., Di Fabrizio L., Maio M., Taribello E., 2004, A&A, 421, 937
Gray R. O., Olsen E. H., 1991, A&AS, 87, 541

Groenewegen M. A. T., 2007, A&A, 474, 975
Groenewegen M. A. T., Udalski A., Bono G., 2008, preprint (arXiv: 0801.2652)
Hindsley R. B., Bell R. A., 1990, ApJ, 348, 673
Janot-Pacheco E., 1976, A&AS, 25, 159
Jones R. V., Carney B. W., Storm J., Latham D. W., 1992, ApJ, 386, 646
Jones R. V., Carney B. W., Fulbright J. P., 1996, PASP, 108, 877
Kiss L. L., 1998, MNRAS, 297, 825
Kiss L. L., Csák B., Thomson J. R., Szatmáry K., 1999, IBVS No. 4660
Laney C. D., 1995, in Stobie R. S., Whitelock P. A., eds, ASP Conf. Ser. Vol. 83, Astrophysical Applications of Stellar Pulsation. Astron. Soc. Pac., San Francisco, p. 367
Laney C. D., Caldwell J. A. R., 2007, MNRAS, 377, 147
Laney C. D., Stobie R. S., 1992, A&AS, 93, 93
Laney C. D., Stobie R. S., 1993, MNRAS, 263, 921
Laney C. D., Stobie R. S., 1995, MNRAS, 274, 337 (LS95)
Lee Y-W., Gim H. B., Casetti-Dinescu D. I., 2007, ApJ, 661, L49
Lloyd Evans T., 1968, MNRAS, 141, 109
Lloyd Evans T., 1980, SAAO Circ., 1, 257
Lloyd Evans T., Wisse P. N. J., Wisse M., 1972, MNRAS, 159, 67
Longmore A. J., Fernley J. A., Jameson R. F., 1986, MNRAS, 220, 279
Luck R. E., Bond H. E., 1989, ApJ, 342, 476
Maas T., Giridhar S., Lambert D. L., 2007, ApJ, 666, 378
Macri L. M., Stanek K. Z., Bersier D., Greenhill L. J., Reid M. J., 2006, ApJ, 652, 1133
Maintz G., 2005, A&A, 442, 381
Mathias P., Gillet D., Fokin A. B., Nardetto N., Kervella P., Mourard D., 2006, A&A, 457, 579
Matsunaga N. et al., 2006, MNRAS, 370, 1979
Merand A. et al., 2005, A&A, 438, L9
Moffett T. J., Barnes T. G., 1984, ApJS, 55, 389
Moore J. H., 1909, Lick Obs. Bull., 5, 111
Nardetto N., Mourard D., Mathias P., Fokin A., Gillet D., 2007, A&A, 471, 661
Nikolov N., Buchantsova N., Frolov. M., 1984, Mean Light Curves of 210 Field RR Lyrae Type Stars. Dept. of Astronomy, Faculty of Physics Astronomical Council of the USSR Academy of Sciences for Department of Astronomy, University of Sofia
Pel J. W., 1976, A&AS, 24, 413
Pojmanski G., 2002, Acta Astron., 52, 397 (ASAS Catalogue)
Popowski P., Gould A., 1998, AJ, 506, 259
Pritzl B. J., Smith H. A., Stetson P. B., Catelan M., Sweigart A. V., Layden A. C., Rich R. M., 2003, AJ, 126, 1381
Rood R. T., 1973, ApJ, 184, 815
Salaris M., Held E. V., Ortolani S., Gullieuszik M., Momany Y., 2007, A&A, 476, 243
Sandage A., Tammann G. A., 2006, ARA&A, 44, 93
Sanwal N. B., Sarma M. B. K., 1991, JA&A, 12, 119
Sasselov D. D., Lester J. B., 1990, ApJ, 362, 333
Schmidt E. G., 1991, AJ, 102, 1766
Shobbrook R. R., 1992, MNRAS, 255, 486
Sollima A., Cacciari C., Valenti E., 2006, MNRAS, 372, 1675
Sollima A., Cacciari C., Arkharov A. A., Larionov V. M., Gorshanov D. L., Efimova N. V., Piersimoni A., 2008, MNRAS, 384, 1583
Stibbs D. W. N., 1955, MNRAS, 115, 363
Stobie R. S., Balona L. A., 1979, MNRAS, 189, 641
Szabados L., 1981, Comm. Konkoly Obs., 77, 1
Szabados L., 1990, MNRAS, 242, 285
Taylor M. M., Booth A. J., 1998, MNRAS, 298, 594
Taylor M. M., Albrow M. D., Booth A. J., Cottrell P. L., 1997, MNRAS, 292, 662
van Leeuwen F., 2007a, *Hipparcos*, the New Reductions of the Raw Data. Springer, Berlin, in press
van Leeuwen F., 2007b, A&A, 474, 653
van Leeuwen F., Feast M. W., Whitelock P. A., Laney C. D., 2007, MNRAS, 379, 723
Wallerstein G., 2002, PASP, 114, 689
Wallerstein G., Gonzalez G., 1996, MNRAS, 282, 1236
Wallerstein G., Jacobsen T. S., Cottrell P. L., Clark M., Albrow M., 1992, MNRAS, 259, 474
Whitelock P. A., Feast M. W., van Leeuwen F., 2008, MNRAS, 386, 313
Wils P., Lloyd C., Bernhardt K., 2006, MNRAS, 368, 1757
Wilson T. D., Carter M. W., Barnes T. G., Van Citters G. W., Moffett T. J., 1989, ApJS, 69, 951
Wisse P. N. J. W. M., 1970, MNSSA, 29, 151
Zucker S., Alexander T., Gillessen S., Eisenhauer F., Genzel R., 2006, ApJ, 639, L21

APPENDIX A: INFRARED PHOTOMETRY

Previously unpublished *JHK* observations for classical Cepheids, ζ Gem and X Sgr, and for the CephIIs, V553 Cen, κ Pav and SW Tau, are given in Table A1. These data were obtained by CDL with the IRP Mk II photometer and 0.75-m telescope at the Sutherland observing station of the South African Astronomical Observatory (SAAO), exactly as for the classical Cepheid data given in Laney & Stobie (1992). This single-channel device was used with a 36-arcsec aperture and a chopping distance of 3 arcmin, and is particularly suited to bright objects. The data are on the SAAO standard system (Carter 1990), which was established with the same telescope, photometer and filter set. Accuracy is typically 0.005–0.008 mag for bright stars, including standardization. Similar data for l Car and β Dor have been taken from Laney & Stobie (1992), while IR data for δ Cep on the CIT system were taken from Barnes et al. (1997) and transformed to the Carter system by the formulae given in Laney & Stobie (1993). For convenience, these data are given in Table A1 as well, with the phases and $V-K$ values calculated for the radius solutions used here.

Table A1. Data for BW solutions.

JD	Phase	K	H	J	$V-K$	L
			δ Cep			
		Period = 5.366 247 50 d, Epoch = 244 8809.6246				
244 8429.980	0.2532	2.250	2.310	2.671	1.621	
244 8430.953	0.4346	2.275	2.346	2.761	1.817	
244 8431.985	0.6269	2.372	2.442	2.885	1.913	
244 8433.888	0.9815	2.301	2.349	2.612	1.219	
244 8434.969	0.1829	2.256	2.310	2.646	1.510	
244 8435.947	0.3652	2.273	2.338	2.732	1.747	
244 8436.958	0.5536	2.320	2.388	2.812	1.888	
244 8437.941	0.7368	2.444	2.521	2.939	1.900	
244 8438.912	0.9177	2.385	2.433	2.732	1.364	
244 8804.979	0.1343	2.254	2.309	2.632	1.439	
244 8805.964	0.3178	2.251	2.325	2.705	1.706	
244 8807.942	0.6864	2.411	2.484	2.917	1.921	
244 8808.930	0.8706	2.429	2.491	2.833	1.589	
244 8864.824	0.2864	2.231	2.296	2.668	1.685	
244 8865.799	0.4681	2.286	2.343	2.763	1.834	
244 8867.941	0.8673	2.434	2.494	2.849	1.601	
244 8870.747	0.3902	2.265	2.312	2.728	1.784	
244 8871.829	0.5918	2.349	2.419	2.847	1.901	
244 8872.920	0.7951	2.458	2.528	2.939	1.837	
244 8873.680	0.9367	2.343	2.393	2.669	1.309	
244 8873.976	0.9919	2.284	2.332	2.586	1.227	
244 9170.983	0.3391	2.250	2.309	2.705	1.736	
244 9172.912	0.6986	2.421	2.493	2.926	1.917	
244 9173.945	0.8911	2.401	2.462	2.783	1.500	
244 9174.952	0.0787	2.264	2.315	2.603	1.347	
244 9175.900	0.2554	2.250	2.311	2.673	1.624	
244 9176.984	0.4574	2.287	2.351	2.760	1.824	

Table A1 – *continued*

JD	Phase	K	H	J	$V-K$	L
X Sgr						
Period = 7.012 6750 d, Epoch = 244 9086.8197						
244 8846.455	0.7242	2.627	2.745	3.189	2.229	
244 8849.447	0.1509	2.451	2.541	2.918	1.928	
244 8850.461	0.2955	2.458	2.558	2.968	2.064	
244 8851.393	0.4284	2.487	2.591	3.025	2.188	
244 8852.429	0.5761	2.549	2.655	3.114	2.279	
244 9263.318	0.1685	2.444	2.541	2.923	1.956	
244 9291.232	0.1490	2.444	2.545	2.907	1.933	
244 9292.231	0.2914	2.452	2.547	2.961	2.068	
244 9534.463	0.8335	2.627	2.724	3.119	2.004	
244 9535.472	0.9773	2.509	2.603	2.927	1.756	
244 9537.453	0.2598	2.438	2.542	2.930	2.064	
244 9538.451	0.4021	2.473	2.572	2.996	2.160	
244 9598.329	0.9407	2.539	2.623	2.951	1.776	
244 9601.312	0.3661	2.469	2.559	2.982	2.111	
244 9859.677	0.2086	2.452	2.538	2.925	2.000	
244 9878.570	0.9028	2.588	2.671	3.015	1.823	
244 9889.482	0.4588	2.496	2.600	3.048	2.227	
244 9890.517	0.6064	2.561	2.667	3.128	2.277	
244 9941.461	0.8709	2.597	2.692	3.060	1.913	
244 9942.472	0.0151	2.478	2.571	2.900	1.782	
245 0142.667	0.5627	2.549	2.656	3.102	2.274	
245 0157.671	0.7023	2.618	2.717	3.165	2.246	
245 0160.679	0.1312	2.453	2.545	2.906	1.904	
245 0682.301	0.5139	2.510	2.612	3.060	2.280	
245 0683.405	0.6714	2.595	2.689	3.148	2.265	
245 0685.354	0.9493	2.516	2.610	2.936	1.783	
245 0912.682	0.3660	2.456	2.554	2.964	2.124	
245 0219.546	0.5256	2.533	2.630	3.088	2.268	
245 0221.553	0.8118	2.631	2.731	3.145	2.066	
245 0240.470	0.5093	2.505	2.622	3.069	2.282	
245 0244.557	0.0921	2.468	2.554	2.911	1.852	
244 9445.690	0.1745	2.444	2.542	2.906	1.965	
244 9590.389	0.8084	2.632	2.727	3.159	2.074	
244 9620.321	0.0767	2.476	2.558	2.910	1.830	
245 0262.466	0.6459	2.593	2.694	3.145	2.258	
245 0262.509	0.6520	2.578	2.692	3.140	2.275	
β Dor						
Period = 9.842 578 d, Epoch = 244 7913.2106						
244 7516.626	0.7072	2.073	2.131	2.537	1.742	
244 7517.537	0.7998	2.044	2.107	2.466	1.640	
244 7518.630	0.9108	1.987	2.041	2.401	1.627	
244 7520.269	0.0774	1.900	1.968	2.358	1.643	
244 7521.605	0.2131	1.856	1.922	2.348	1.825	
244 7522.287	0.2824	1.877	1.945	2.381	1.911	
244 7524.511	0.5084	1.994	2.070	2.531	2.087	
244 7525.362	0.5948	2.054	2.134	2.579	1.981	
244 7526.346	0.6948	2.057	2.136	2.531	1.772	
244 7528.533	0.9170	1.983	2.049	2.419	1.622	
244 7534.370	0.5100	1.995	2.076	2.562	2.086	1.894
244 7567.352	0.8610	2.010	2.076	2.448	1.637	
244 7570.367	0.1673	1.869	1.929	2.323	1.760	
244 7604.320	0.6169	2.055	2.136	2.560	1.948	
244 7607.269	0.9165	1.982	2.044	2.415	1.623	
244 7642.251	0.4707	1.979	2.050	2.528	2.072	
244 7643.229	0.5700	2.045	2.124	2.589	2.008	
244 7644.221	0.6708	2.058	2.132	2.531	1.811	
244 7645.203	0.7706	2.051	2.107	2.488	1.680	
244 7646.194	0.8713	1.998	2.070	2.450	1.646	
244 7647.249	0.9785	1.918	1.988	2.330	1.535	
244 7660.204	0.2947	1.883	1.948	2.380	1.924	1.790
244 7670.194	0.3097	1.892	1.955	2.408	1.935	
244 7675.187	0.8169	2.023	2.088	2.459	1.643	
244 7676.193	0.9192	1.982	2.048	2.422	1.619	
244 7713.698	0.7296	2.054	2.137	2.514	1.739	
244 7714.684	0.8298	2.009	2.085	2.455	1.649	
244 7715.727	0.9358	1.972	2.037	2.371	1.592	
244 7716.716	0.0363	1.902	1.980	2.316	1.577	
244 7719.719	0.3414	1.891	1.972	2.420	1.982	
244 7727.698	0.1520	1.875	1.940	2.330	1.731	
244 7731.687	0.5573	2.041	2.113	2.589	2.019	
244 7742.689	0.6751	2.062	2.135	2.538	1.798	
244 7744.673	0.8767	2.003	2.067	2.445	1.639	1.897
244 7759.672	0.4006	1.923	2.001	2.473	2.047	1.823
244 7769.689	0.4183	1.941	2.009	2.494	2.048	
244 7803.622	0.8659	2.001	2.071	2.436	1.645	
244 7811.633	0.6798	2.058	2.134	2.533	1.793	
244 7815.547	0.0774	1.904	1.962	2.343	1.639	1.800
244 7816.620	0.1865	1.868	1.939	2.347	1.785	1.770
244 7821.586	0.6910	2.061	2.129	2.528	1.772	1.954
244 7823.528	0.8883	1.996	2.057	2.443	1.641	1.903
ζ Gem						
Period = 10.149 92 d, Epoch = 245 0180.19683						
244 8317.332	0.4651	2.142	2.228	2.697	2.029	
244 8318.339	0.5643	2.205	2.278	2.730	1.944	
244 8320.323	0.7598	2.200	2.266	2.655	1.689	
244 9789.295	0.4872	2.157	2.238	2.703	2.022	
244 9790.260	0.5823	2.209	2.292	2.724	1.919	
245 0079.492	0.0783	2.076	2.149	2.523	1.653	
245 0082.476	0.3723	2.103	2.185	2.648	1.982	
245 0147.267	0.7557	2.192	2.268	2.656	1.701	
245 0149.304	0.9563	2.118	2.171	2.541	1.589	
245 0150.279	0.0524	2.085	2.140	2.522	1.626	
245 0151.269	0.1499	2.057	2.121	2.528	1.742	
245 0152.253	0.2469	2.054	2.120	2.551	1.867	
245 0155.274	0.5445	2.192	2.278	2.732	1.974	
245 0156.300	0.6456	2.220	2.287	2.697	1.815	
245 0157.270	0.7412	2.207	2.277	2.659	1.700	
245 0158.257	0.8384	2.163	2.225	2.597	1.651	
245 0159.274	0.9386	2.127	2.183	2.551	1.591	
245 0160.283	0.0380	2.080	2.142	2.509	1.623	
245 0161.268	0.1351	2.049	2.115	2.511	1.734	
245 0471.427	0.6929	2.208	2.282	2.680	1.757	
245 0472.418	0.7905	2.192	2.256	2.635	1.668	
245 0473.400	0.8872	2.140	2.212	2.573	1.624	
245 0474.396	0.9854	2.096	2.154	2.517	1.600	
245 0475.397	0.0840	2.058	2.144	2.509	1.675	
245 0476.386	0.1814	2.050	2.121	2.532	1.787	
245 0824.411	0.4699	2.165	2.236	2.705	2.009	
245 0827.407	0.7651	2.192	2.260	2.637	1.692	
245 0886.262	0.5636	2.196	2.284	2.722	1.953	
245 1155.527	0.0924	2.065	2.127	2.522	1.676	
245 1177.479	0.2552	2.072	2.141	2.584	1.860	
ℓ Car						
Period = 35.543 270 d, Epoch = 244 6104.2086						
244 6575.359	0.2557	0.973	1.088	1.656	2.684	
244 6576.304	0.2823	0.971	1.088	1.659	2.719	
244 6597.218	0.8707	1.286	1.383	1.904	2.467	1.119
244 6601.246	0.9840	1.129	1.242	1.694	2.225	
244 6603.261	0.0407	1.069	1.185	1.662	2.300	
244 6607.256	0.1531	1.012	1.118	1.648	2.509	
244 6609.251	0.2092	0.975	1.081	1.635	2.624	
244 6610.264	0.2377	0.990	1.097	1.642	2.645	
244 6611.230	0.2649	0.978	1.099	1.662	2.690	
244 6740.634	0.9057	1.220	1.341	1.812	2.345	
244 6741.617	0.9333	1.183	1.289	1.755	2.265	

Table A1 – *continued*

JD	Phase	K	H	J	$V-K$	L
244 6758.567	0.4102	1.007	1.133	1.736	2.867	0.843
244 6782.560	0.0852	1.033	1.157	1.652	2.387	0.924
244 6803.518	0.6749	1.150	1.280	1.879	2.917	0.980
244 6834.413	0.5441	1.077	1.202	1.828	2.954	0.903
244 6862.546	0.3356	0.985	1.099	1.682	2.787	
244 6863.548	0.3638	0.983	1.108	1.702	2.834	
244 6880.261	0.8340	1.274	1.396	1.938	2.651	
244 6881.505	0.8690	1.275	1.398	1.899	2.487	
244 6886.494	0.0094	1.098	1.210	1.664	2.253	
244 6898.356	0.3431	0.978	1.086	1.675	2.806	0.817
244 6899.341	0.3708	0.974	1.099	1.698	2.854	0.826
244 6914.315	0.7921	1.267	1.394	1.964	2.756	1.126
244 6915.396	0.8225	1.274	1.403	1.966	2.689	1.129
244 6967.254	0.2815	0.946	1.071	1.637	2.743	0.830
244 6972.286	0.4231	1.010	1.129	1.726	2.876	
244 6978.260	0.5912	1.110	1.243	1.863	2.944	
244 6981.247	0.6752	1.192	1.318	1.907	2.874	
244 6982.239	0.7031	1.207	1.334	1.932	2.856	
244 6983.240	0.7313	1.229	1.352	1.936	2.826	
244 6985.207	0.7866	1.282	1.398	1.961	2.748	1.131
κ Pav						
Period = 9.0814 d, Epoch = 244 6684.0691						
244 5928.495	0.7998	3.039	3.102	3.396	1.399	
244 5929.486	0.9089	2.816	2.886	3.149	1.177	2.778
244 5953.440	0.5466	2.861	2.945	3.355	1.896	
244 6329.287	0.9331	2.799	2.856	3.105	1.154	
244 6345.338	0.7006	3.041	3.110	3.465	1.594	
244 6652.532	0.5273	2.859	2.934	3.354	1.893	
244 6675.477	0.0539	2.673	2.733	3.013	1.275	
244 6676.465	0.1627	2.646	2.715	3.045	1.518	
244 6680.420	0.5982	2.924	3.003	3.405	1.821	
244 6682.439	0.8205	3.012	3.067	3.353	1.330	
244 6684.440	0.0408	2.680	2.750	3.033	1.252	
244 6686.435	0.2605	2.654	2.732	3.111	1.740	
244 6694.370	0.1343	2.639	2.706	3.026	1.463	2.584
244 6703.267	0.1140	2.667	2.730	3.051	1.391	2.612
244 6739.269	0.0783	2.656	2.725	3.001	1.331	
244 6740.278	0.1895	2.645	2.716	3.058	1.580	
244 6741.275	0.2992	2.669	2.745	3.136	1.801	
244 6744.251	0.6269	2.952	3.019	3.420	1.763	2.868
244 6748.245	0.0667	2.666	2.721	3.005	1.301	
244 6970.642	0.5560	2.875	2.953	3.366	1.883	
244 7029.481	0.0351	2.695	2.757	3.037	1.232	
244 7078.344	0.4157	2.737	2.818	3.238	1.942	
244 7646.640	0.9937	2.761	2.814	3.063	1.151	
244 7713.603	0.3673	2.729	2.802	3.202	1.863	
244 7715.598	0.5870	2.924	3.001	3.411	1.828	
V553 Cen						
Period = 2.060 464 d, Epoch = 244 8437.115 40						
244 6688.236	0.2206	6.755	6.851	7.180	1.631	
244 6864.611	0.8203	6.974	7.053	7.357	1.452	
244 6868.439	0.6781	6.992	7.083	7.408	1.595	
244 6881.644	0.0868	6.789	6.860	7.153	1.470	
244 6882.647	0.5736	6.973	7.073	7.431	1.725	
244 6886.628	0.5057	6.919	7.013	7.386	1.815	
244 6888.626	0.4754	6.900	6.991	7.367	1.814	
244 6890.616	0.4412	6.874	6.973	7.350	1.801	
244 6892.610	0.4089	6.852	6.939	7.309	1.782	
244 6978.388	0.0394	6.809	6.887	7.171	1.422	
244 6980.413	0.0222	6.819	6.893	7.186	1.407	
244 6981.365	0.4842	6.905	6.998	7.377	1.817	
244 6982.367	0.9705	6.862	6.942	7.223	1.365	
244 7029.269	0.7333	7.004	7.094	7.414	1.562	
244 7252.552	0.0987	6.784	6.858	7.155	1.485	

Table A1 – *continued*

JD	Phase	K	H	J	$V-K$	L
244 7602.594	0.9838	6.853	6.929	7.215	1.372	
244 7642.484	0.3435	6.810	6.906	7.260	1.742	
244 7643.521	0.8468	6.957	7.034	7.328	1.409	
244 7645.485	0.7999	6.990	7.064	7.365	1.481	
244 7646.482	0.2838	6.791	6.871	7.220	1.676	
244 7647.535	0.7949	6.989	7.067	7.371	1.493	
244 7674.414	0.8400	6.929	7.021	7.323	1.452	
244 7675.431	0.3336	6.795	6.881	7.239	1.743	
244 7676.431	0.8189	6.976	7.058	7.351	1.453	
244 7714.362	0.2278	6.775	6.861	7.196	1.619	
244 7716.363	0.1990	6.766	6.849	7.180	1.597	
244 7717.367	0.6863	7.005	7.083	7.411	1.579	
244 7771.267	0.8454	6.973	7.029	7.332	1.396	
SW Tau						
Period = 1.583 565 d, Epoch = 244 5013.2696						
244 5950.650	0.9431	7.903	7.997	8.238	1.462	
244 5953.656	0.8414	7.979	8.065	8.286	1.414	
244 5954.643	0.4646	7.978	8.102	8.460	2.006	
244 6023.497	0.9450	7.897	7.988	8.239	1.467	
244 6024.407	0.5197	8.015	8.120	8.500	2.028	
244 6069.412	0.9397	7.896	7.990	8.245	1.472	
244 6073.364	0.4354	7.982	8.056	8.424	1.960	
244 6075.340	0.6832	8.173	8.262	8.588	1.892	
244 6326.631	0.3701	7.921	8.028	8.392	1.930	
244 6326.654	0.3846	7.919	8.020	8.382	1.951	
244 6334.623	0.4169	7.925	8.018	8.360	1.990	
244 6335.654	0.0680	7.857	7.945	8.200	1.553	
244 6338.664	0.9687	7.885	7.983	8.216	1.466	
244 6345.613	0.3569	7.920	8.012	8.364	1.915	
244 6363.537	0.6757	8.154	8.257	8.592	1.913	
244 6427.296	0.9387	7.919	7.986	8.224	1.449	
244 6664.636	0.8157	8.010	8.095	8.359	1.439	
244 6676.646	0.3998	7.933	8.027	8.384	1.957	
244 6677.645	0.0307	7.878	7.939	8.195	1.478	
244 6682.640	0.1850	7.905	7.991	8.319	1.768	
244 6686.649	0.7166	8.176	8.266	8.602	1.857	
244 6693.609	0.1117	7.890	7.984	8.283	1.614	
244 6702.618	0.8008	8.061	8.117	8.380	1.462	
244 6739.479	0.0780	7.878	7.968	8.237	1.552	
244 6740.568	0.7657	8.100	8.196	8.492	1.679	
244 6741.614	0.4262	7.937	8.063	8.411	1.991	
244 6744.481	0.2367	7.903	8.005	8.325	1.825	
244 6745.469	0.8606	7.959	8.045	8.295	1.431	
244 6746.536	0.5344	8.044	8.155	8.501	2.010	
244 6747.484	0.1331	7.881	7.978	8.267	1.673	
244 6748.506	0.7784	8.086	8.154	8.421	1.594	
244 6780.359	0.8932	7.942	8.057	8.283	1.454	
244 6783.391	0.8079	8.010	8.094	8.335	1.474	
244 6829.294	0.7950	8.042	8.127	8.383	1.517	
244 7023.659	0.5339	8.048	8.142	8.509	2.006	
244 7072.590	0.4331	7.951	8.053	8.425	1.987	
244 7077.644	0.6247	8.109	8.194	8.571	1.989	
244 7148.376	0.2910	7.911	8.007	8.333	1.853	
244 7431.631	0.1627	7.904	8.010	8.287	1.721	
244 7211.649	0.2470	7.891	7.996	8.346	1.843	
244 7212.640	0.8728	7.954	8.043	8.267	1.440	
244 7212.644	0.8754	7.948	8.034	8.273	1.447	
244 7212.661	0.8861	7.950	8.027	8.271	1.446	
244 7212.664	0.8880	7.946	8.034	8.273	1.450	
244 7212.706	0.9145	7.925	8.015	8.257	1.461	
244 7212.709	0.9164	7.919	8.015	8.253	1.466	
244 7219.617	0.2787	7.882	7.988	8.344	1.871	
244 7219.621	0.2812	7.884	7.990	8.333	1.871	
244 7219.678	0.3172	7.914	8.003	8.329	1.876	

Table A1 – *continued*

JD	Phase	K	H	J	$V-K$	L
244 7219.710	0.3374	7.903	8.007	8.349	1.910	
244 7220.655	0.9342	7.912	8.009	8.247	1.460	
244 7460.892	0.6406	8.125	8.228	8.570	1.962	
244 7460.974	0.6924	8.146	8.252	8.583	1.915	
244 7461.017	0.7196	8.171	8.274	8.601	1.855	
244 7462.792	0.8405	7.986	8.052	8.297	1.407	
244 7462.990	0.9655	7.902	7.986	8.221	1.450	
244 7465.796	0.7374	8.157	8.249	8.571	1.805	
244 7465.846	0.7690	8.101	8.193	8.485	1.652	
244 7465.921	0.8164	8.021	8.094	8.325	1.425	
244 7465.983	0.8555	7.955	8.044	8.281	1.434	
244 7466.023	0.8808	7.960	8.049	8.275	1.436	
244 7466.764	0.3487	7.922	8.019	8.356	1.904	
244 7466.828	0.3891	7.921	8.039	8.378	1.955	
244 7466.868	0.4144	7.947	8.050	8.401	1.964	
244 7466.906	0.4384	7.965	8.059	8.425	1.981	
244 7466.944	0.4624	7.987	8.073	8.434	1.994	
244 7466.985	0.4883	7.997	8.093	8.457	2.018	
244 7467.026	0.5142	8.028	8.134	8.486	2.011	
244 7468.838	0.6584	8.123	8.224	8.580	1.952	
244 7468.995	0.7576	8.110	8.208	8.531	1.729	
244 7469.019	0.7727	8.096	8.179	8.479	1.629	

APPENDIX B: THE DERIVATION OF MEAN JHK_s MAGNITUDES FOR RR LYRAE STARS WITH 2MASS MAGNITUDES

The 2MASS catalogue (Cutri et al. 2003) gives JHK_s magnitudes for a single JD. The derivation of the mean magnitudes (hereafter $\langle J\rangle$, $\langle H\rangle$, $\langle K_s\rangle$) requires (i) ephemerides for each star that will give a phase for the 2MASS data that is accurate to at least 0.1, (ii) a visual amplitude (ΔV) for the RR Lyrae star and (iii) a standard light curve (or template) in each of J, H and K_s which may be converted to the J, H and K_s light curves of the star in question by means of its ΔV. Jones, Carney & Fulbright (1996) gave templates of $K - \langle K\rangle$ *versus* phase for a number of ranges of their B amplitude for type *ab* RR Lyrae stars; a single template was given for type *c* variables. The method that we describe below covers J, H and K_s and gives tables (rather than plots) from which the mean magnitudes can be computed.

B1 Procedure and results

B1.1 Ephemerides and visual amplitudes

The 2MASS observations were made in the period 1997–2000. We therefore need to get a time of maximum light [JD(max)] for each variable that is as near to this epoch as possible. Fortunately, a JD(max) for most of our variables can be found either in the ASAS catalogue (Pojmanski 2002) which covers the sky south of declination $+28°$ with epochs since 1997 or in the compilation by Wils, Lloyd & Bernhardt (2006) for epochs 1999–2000 for stars north of declination $-38°$. In other cases, recent values of JD(max) are cited by Maintz (2005). Periods were primarily taken from the ASAS catalogue (loc. cit.) or Maintz (loc. cit.). The majority of the values of ΔV were taken from the catalogue of Nikolov, Buchantsova & Frolov. (1984), the ASAS catalogue (loc. cit.) or Schmidt (1991). In some cases, the *Hipparcos* amplitude was multiplied by 0.874 to get ΔV. These data allowed us to derive both the phase of the 2MASS data and ΔV for each variable.

B1.2 A standard RR Lyrae light curve for J, H and K_s

Jones et al. (1996) noted that the RR*ab* K light curves showed small differences in their shapes that were a function of amplitude. They therefore provided templates of $K - \langle K\rangle$ as a function of phase (ϕ) for stars in five different ranges of B amplitude. These templates were derived from the K light curves of field RR Lyrae stars that had been observed by several authors. We chose to produce a template of a single well-observed RR Lyrae star (SW And) of intermediate amplitude. Excellent light curves in J, H and K have been given for SW And by Barnes, Moffett & Freuh (1992). These were based on observations made in 1988; they also gave *BVRI* data for the same year. Jones et al. (1992) gave a partial *KBV* light curve for SW And based on observations made in 1987. In addition, 31 unpublished observations in H made by Kinman between 1987 November and 1989 November were also available. All these IR observations were made using the Kitt Peak 1.3-m telescope and are shown in Fig. B1 using the ephemeris:

$$\mathrm{JD(max)} = 244\,430\,67.6819 + 0.442\,265\,82E. \qquad \text{(B1)}$$

The agreement between the three data sets shows that the light curve is stable. The 2MASS observations were made 12 yr later (JD = 244 507 39.8477) and the phase (0.426) was determined from an

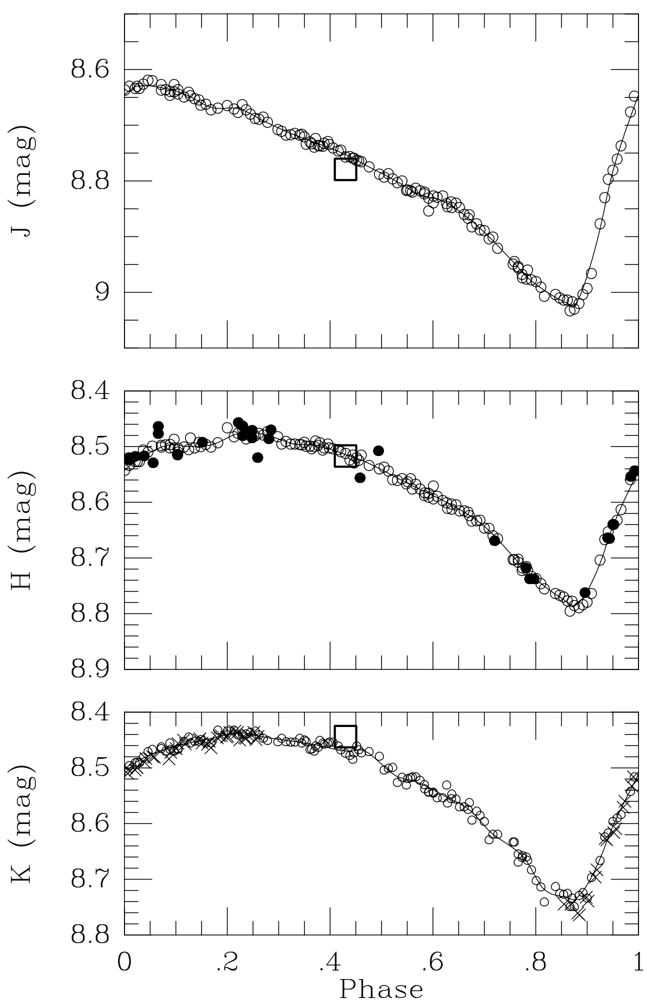

Figure B1. The *JHK* light curves of SW And. The open circles are from observations of Barnes et al. (1992), the crosses from those of Jones et al. (1992) and the filled circles are Kinman's unpublished observations. The 2MASS observations are shown as the large open squares.

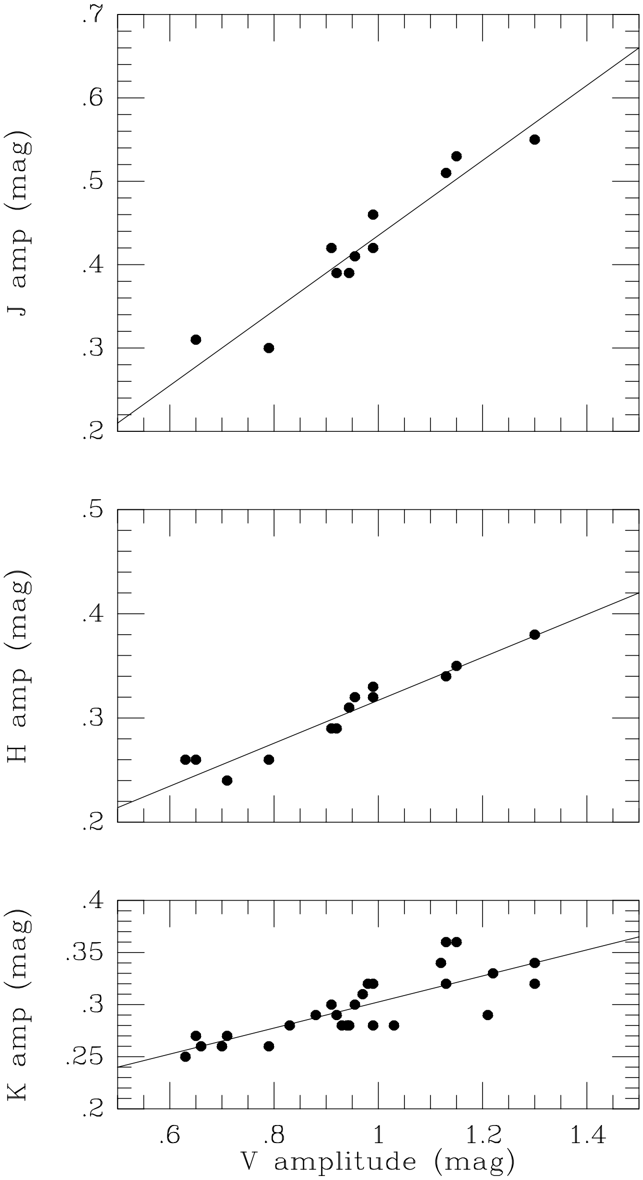

Figure B2. The relation between the J, H and K amplitudes and their V amplitudes for RR Lyrae stars that have well determined light curves.

ephemeris derived from the period given by Maintz (2005) and the JD (max) given by Wils et al. (2006):

$$\mathrm{JD(max)} = 244\,514\,16.3203 + 0.442\,262E. \quad \text{(B2)}$$

The 2MASS observations (open squares) show good agreement with the light curves given in Fig. B1. The intensity-weighted $\langle J\rangle$, $\langle H\rangle$ and $\langle K\rangle$ of SW And are 8.780, 8.575 and 8.575, respectively. The corrections to be applied to the J, H and K magnitudes of this star as a function of phase to get the intensity-weighted mean magnitudes are given in Table B1. These corrections must be multiplied by a factor which takes into account the difference between the amplitude ΔV of SW And and that of the variable under consideration.

B1.3 The correction for the amplitude of the variable

A literature search for RR*ab* Lyrae stars with reliable IR light curves gave 11, 13 and 27 with J, H and K amplitudes, respectively. These

Table B1. Corrections to *JHK* as a function of phase.

Phase	J	ΔJ	H	ΔH	K	ΔK
0.0000	8.6450	0.1350	8.5420	0.0330	8.5110	0.0210
0.0050	8.6415	0.1385	8.5383	0.0367	8.5061	0.0259
0.0100	8.6376	0.1424	8.5345	0.0405	8.5010	0.0310
0.0150	8.6339	0.1461	8.5308	0.0442	8.4960	0.0360
0.0200	8.6311	0.1489	8.5274	0.0476	8.4917	0.0403
0.0250	8.6299	0.1501	8.5245	0.0505	8.4884	0.0436
0.0300	8.6294	0.1506	8.5217	0.0533	8.4858	0.0462
0.0350	8.6291	0.1509	8.5189	0.0561	8.4834	0.0486
0.0400	8.6291	0.1509	8.5161	0.0589	8.4811	0.0509
0.0450	8.6292	0.1508	8.5134	0.0616	8.4789	0.0531
0.0500	8.6296	0.1504	8.5107	0.0643	8.4769	0.0551
0.0550	8.6300	0.1500	8.5081	0.0669	8.4750	0.0570
0.0600	8.6306	0.1494	8.5057	0.0693	8.4731	0.0589
0.0650	8.6313	0.1487	8.5035	0.0715	8.4714	0.0606
0.0700	8.6321	0.1479	8.5015	0.0735	8.4697	0.0623
0.0750	8.6330	0.1470	8.4997	0.0753	8.4680	0.0640
0.0800	8.6338	0.1462	8.4983	0.0767	8.4663	0.0657
0.0850	8.6348	0.1452	8.4972	0.0778	8.4647	0.0673
0.0900	8.6359	0.1441	8.4968	0.0782	8.4632	0.0688
0.0950	8.6372	0.1428	8.4969	0.0781	8.4619	0.0701
0.1000	8.6387	0.1413	8.4973	0.0777	8.4607	0.0713
0.1050	8.6403	0.1397	8.4979	0.0771	8.4595	0.0725
0.1100	8.6420	0.1380	8.4986	0.0764	8.4584	0.0736
0.1150	8.6438	0.1362	8.4993	0.0757	8.4573	0.0747
0.1200	8.6457	0.1343	8.4998	0.0752	8.4563	0.0757
0.1250	8.6476	0.1324	8.5000	0.0750	8.4552	0.0768
0.1300	8.6497	0.1303	8.5000	0.0750	8.4542	0.0778
0.1350	8.6521	0.1279	8.5000	0.0750	8.4532	0.0788
0.1400	8.6547	0.1253	8.4999	0.0751	8.4522	0.0798
0.1450	8.6575	0.1225	8.4998	0.0752	8.4513	0.0807
0.1500	8.6602	0.1198	8.4996	0.0754	8.4504	0.0816
0.1550	8.6627	0.1173	8.4993	0.0757	8.4495	0.0825
0.1600	8.6650	0.1150	8.4987	0.0763	8.4486	0.0834
0.1650	8.6669	0.1131	8.4979	0.0771	8.4477	0.0843
0.1700	8.6682	0.1118	8.4967	0.0783	8.4468	0.0852
0.1750	8.6691	0.1109	8.4952	0.0798	8.4458	0.0862
0.1800	8.6695	0.1105	8.4934	0.0816	8.4447	0.0873
0.1850	8.6697	0.1103	8.4913	0.0837	8.4435	0.0885
0.1900	8.6697	0.1103	8.4891	0.0859	8.4424	0.0896
0.1950	8.6695	0.1105	8.4868	0.0882	8.4412	0.0908
0.2000	8.6693	0.1107	8.4845	0.0905	8.4401	0.0919
0.2050	8.6692	0.1108	8.4822	0.0928	8.4391	0.0929
0.2100	8.6693	0.1107	8.4802	0.0948	8.4383	0.0937
0.2150	8.6695	0.1105	8.4784	0.0966	8.4376	0.0944
0.2200	8.6702	0.1098	8.4769	0.0981	8.4372	0.0948
0.2250	8.6713	0.1087	8.4758	0.0992	8.4370	0.0950
0.2300	8.6728	0.1072	8.4751	0.0999	8.4372	0.0948
0.2350	8.6747	0.1053	8.4747	0.1003	8.4377	0.0943
0.2400	8.6769	0.1031	8.4746	0.1004	8.4384	0.0936
0.2450	8.6793	0.1007	8.4746	0.1004	8.4394	0.0926
0.2500	8.6819	0.0981	8.4749	0.1001	8.4405	0.0915
0.2550	8.6845	0.0955	8.4754	0.0996	8.4416	0.0904
0.2600	8.6872	0.0928	8.4760	0.0990	8.4427	0.0893
0.2650	8.6897	0.0903	8.4768	0.0982	8.4438	0.0882
0.2700	8.6921	0.0879	8.4776	0.0974	8.4447	0.0873
0.2750	8.6943	0.0857	8.4786	0.0964	8.4454	0.0866
0.2800	8.6965	0.0835	8.4799	0.0951	8.4461	0.0859
0.2850	8.6987	0.0813	8.4813	0.0937	8.4468	0.0852
0.2900	8.7008	0.0792	8.4830	0.0920	8.4474	0.0846
0.2950	8.7030	0.0770	8.4848	0.0902	8.4480	0.0840
0.3000	8.7051	0.0749	8.4866	0.0884	8.4486	0.0834
0.3050	8.7072	0.0728	8.4884	0.0866	8.4492	0.0828
0.3100	8.7092	0.0708	8.4902	0.0848	8.4498	0.0822
0.3150	8.7113	0.0687	8.4919	0.0831	8.4504	0.0816

Table B1 – *continued*

Phase	J	ΔJ	H	ΔH	K	ΔK
0.3200	8.7133	0.0667	8.4933	0.0817	8.4511	0.0809
0.3250	8.7152	0.0648	8.4946	0.0804	8.4517	0.0803
0.3300	8.7171	0.0629	8.4955	0.0795	8.4524	0.0796
0.3350	8.7189	0.0611	8.4961	0.0789	8.4531	0.0789
0.3400	8.7207	0.0593	8.4964	0.0786	8.4538	0.0782
0.3450	8.7224	0.0576	8.4965	0.0785	8.4545	0.0775
0.3500	8.7240	0.0560	8.4966	0.0784	8.4552	0.0768
0.3550	8.7256	0.0544	8.4966	0.0784	8.4559	0.0761
0.3600	8.7273	0.0527	8.4966	0.0784	8.4567	0.0753
0.3650	8.7289	0.0511	8.4969	0.0781	8.4575	0.0745
0.3700	8.7306	0.0494	8.4974	0.0776	8.4583	0.0737
0.3750	8.7324	0.0476	8.4982	0.0768	8.4592	0.0728
0.3800	8.7341	0.0459	8.4992	0.0758	8.4601	0.0719
0.3850	8.7358	0.0442	8.5004	0.0746	8.4612	0.0708
0.3900	8.7376	0.0424	8.5018	0.0732	8.4623	0.0697
0.3950	8.7393	0.0407	8.5032	0.0718	8.4634	0.0686
0.4000	8.7410	0.0390	8.5047	0.0703	8.4646	0.0674
0.4050	8.7428	0.0372	8.5063	0.0687	8.4657	0.0663
0.4100	8.7446	0.0354	8.5079	0.0671	8.4668	0.0652
0.4150	8.7465	0.0335	8.5095	0.0655	8.4678	0.0642
0.4200	8.7484	0.0316	8.5111	0.0639	8.4687	0.0633
0.4250	8.7504	0.0296	8.5127	0.0623	8.4695	0.0625
0.4300	8.7524	0.0276	8.5143	0.0607	8.4701	0.0619
0.4350	8.7546	0.0254	8.5158	0.0592	8.4702	0.0618
0.4400	8.7570	0.0230	8.5173	0.0577	8.4697	0.0623
0.4450	8.7594	0.0206	8.5189	0.0561	8.4689	0.0631
0.4500	8.7619	0.0181	8.5205	0.0545	8.4682	0.0638
0.4550	8.7645	0.0155	8.5221	0.0529	8.4678	0.0642
0.4600	8.7670	0.0130	8.5239	0.0511	8.4679	0.0641
0.4650	8.7695	0.0105	8.5258	0.0492	8.4689	0.0631
0.4700	8.7720	0.0080	8.5278	0.0472	8.4709	0.0611
0.4750	8.7744	0.0056	8.5300	0.0450	8.4737	0.0583
0.4800	8.7768	0.0032	8.5322	0.0428	8.4770	0.0550
0.4850	8.7791	0.0009	8.5345	0.0405	8.4808	0.0512
0.4900	8.7815	−0.0015	8.5368	0.0382	8.4848	0.0472
0.4950	8.7839	−0.0039	8.5392	0.0358	8.4891	0.0429
0.5000	8.7863	−0.0063	8.5415	0.0335	8.4934	0.0386
0.5050	8.7887	−0.0087	8.5440	0.0310	8.4977	0.0343
0.5100	8.7911	−0.0111	8.5464	0.0286	8.5019	0.0301
0.5150	8.7935	−0.0135	8.5488	0.0262	8.5058	0.0262
0.5200	8.7960	−0.0160	8.5512	0.0238	8.5093	0.0227
0.5250	8.7985	−0.0185	8.5535	0.0215	8.5124	0.0196
0.5300	8.8011	−0.0211	8.5559	0.0191	8.5150	0.0170
0.5350	8.8038	−0.0238	8.5582	0.0168	8.5170	0.0150
0.5400	8.8067	−0.0267	8.5606	0.0144	8.5186	0.0134
0.5450	8.8095	−0.0295	8.5629	0.0121	8.5199	0.0121
0.5500	8.8124	−0.0324	8.5653	0.0097	8.5210	0.0110
0.5550	8.8152	−0.0352	8.5676	0.0074	8.5221	0.0099
0.5600	8.8179	−0.0379	8.5700	0.0050	8.5232	0.0088
0.5650	8.8205	−0.0405	8.5723	0.0027	8.5244	0.0076
0.5700	8.8228	−0.0428	8.5746	0.0004	8.5259	0.0061
0.5750	8.8248	−0.0448	8.5769	−0.0019	8.5278	0.0042
0.5800	8.8264	−0.0464	8.5792	−0.0042	8.5298	0.0022
0.5850	8.8277	−0.0477	8.5814	−0.0064	8.5320	0.0000
0.5900	8.8287	−0.0487	8.5836	−0.0086	8.5343	−0.0023
0.5950	8.8297	−0.0497	8.5857	−0.0107	8.5366	−0.0046
0.6000	8.8306	−0.0506	8.5879	−0.0129	8.5390	−0.0070
0.6050	8.8316	−0.0516	8.5901	−0.0151	8.5415	−0.0095
0.6100	8.8328	−0.0528	8.5924	−0.0174	8.5440	−0.0120
0.6150	8.8343	−0.0543	8.5947	−0.0197	8.5465	−0.0145
0.6200	8.8361	−0.0561	8.5970	−0.0220	8.5490	−0.0170
0.6250	8.8384	−0.0584	8.5995	−0.0245	8.5515	−0.0195
0.6300	8.8410	−0.0610	8.6019	−0.0269	8.5538	−0.0218
0.6350	8.8438	−0.0638	8.6043	−0.0293	8.5561	−0.0241

Table B1 – *continued*

Phase	J	ΔJ	H	ΔH	K	ΔK
0.6400	8.8468	−0.0668	8.6067	−0.0317	8.5583	−0.0263
0.6450	8.8499	−0.0699	8.6092	−0.0342	8.5606	−0.0286
0.6500	8.8533	−0.0733	8.6117	−0.0367	8.5630	−0.0310
0.6550	8.8567	−0.0767	8.6143	−0.0393	8.5655	−0.0335
0.6600	8.8602	−0.0802	8.6170	−0.0420	8.5683	−0.0363
0.6650	8.8639	−0.0839	8.6198	−0.0448	8.5713	−0.0393
0.6700	8.8675	−0.0875	8.6228	−0.0478	8.5746	−0.0426
0.6750	8.8712	−0.0912	8.6259	−0.0509	8.5783	−0.0463
0.6800	8.8752	−0.0952	8.6291	−0.0541	8.5827	−0.0507
0.6850	8.8792	−0.0992	8.6324	−0.0574	8.5877	−0.0557
0.6900	8.8834	−0.1034	8.6358	−0.0608	8.5929	−0.0609
0.6950	8.8878	−0.1078	8.6394	−0.0644	8.5983	−0.0663
0.7000	8.8922	−0.1122	8.6432	−0.0682	8.6037	−0.0717
0.7050	8.8967	−0.1167	8.6472	−0.0722	8.6088	−0.0768
0.7100	8.9013	−0.1213	8.6514	−0.0764	8.6135	−0.0815
0.7150	8.9058	−0.1258	8.6558	−0.0808	8.6176	−0.0856
0.7200	8.9104	−0.1304	8.6605	−0.0855	8.6213	−0.0893
0.7250	8.9151	−0.1351	8.6654	−0.0904	8.6247	−0.0927
0.7300	8.9199	−0.1399	8.6705	−0.0955	8.6279	−0.0959
0.7350	8.9246	−0.1446	8.6757	−0.1007	8.6309	−0.0989
0.7400	8.9295	−0.1495	8.6810	−0.1060	8.6339	−0.1019
0.7450	8.9343	−0.1543	8.6863	−0.1113	8.6369	−0.1049
0.7500	8.9392	−0.1592	8.6916	−0.1166	8.6399	−0.1079
0.7550	8.9441	−0.1641	8.6969	−0.1219	8.6431	−0.1111
0.7600	8.9490	−0.1690	8.7020	−0.1270	8.6466	−0.1146
0.7650	8.9541	−0.1741	8.7070	−0.1320	8.6503	−0.1183
0.7700	8.9597	−0.1797	8.7119	−0.1369	8.6543	−0.1223
0.7750	8.9652	−0.1852	8.7167	−0.1417	8.6591	−0.1271
0.7800	8.9701	−0.1901	8.7211	−0.1461	8.6647	−0.1327
0.7850	8.9743	−0.1943	8.7254	−0.1504	8.6716	−0.1396
0.7900	8.9782	−0.1982	8.7296	−0.1546	8.6795	−0.1475
0.7950	8.9819	−0.2019	8.7337	−0.1587	8.6880	−0.1560
0.8000	8.9855	−0.2055	8.7378	−0.1628	8.6964	−0.1644
0.8050	8.9890	−0.2090	8.7418	−0.1668	8.7045	−0.1725
0.8100	8.9922	−0.2122	8.7456	−0.1706	8.7115	−0.1795
0.8150	8.9954	−0.2154	8.7493	−0.1743	8.7171	−0.1851
0.8200	8.9984	−0.2184	8.7528	−0.1778	8.7211	−0.1891
0.8250	9.0015	−0.2215	8.7564	−0.1814	8.7240	−0.1920
0.8300	9.0044	−0.2244	8.7598	−0.1848	8.7262	−0.1942
0.8350	9.0073	−0.2273	8.7631	−0.1881	8.7277	−0.1957
0.8400	9.0100	−0.2300	8.7664	−0.1914	8.7288	−0.1968
0.8450	9.0125	−0.2325	8.7695	−0.1945	8.7296	−0.1976
0.8500	9.0149	−0.2349	8.7725	−0.1975	8.7304	−0.1984
0.8550	9.0169	−0.2369	8.7754	−0.2004	8.7313	−0.1993
0.8600	9.0189	−0.2389	8.7782	−0.2032	8.7326	−0.2006
0.8650	9.0217	−0.2417	8.7817	−0.2067	8.7346	−0.2026
0.8700	9.0240	−0.2440	8.7848	−0.2098	8.7364	−0.2044
0.8750	9.0235	−0.2435	8.7860	−0.2110	8.7366	−0.2046
0.8800	9.0180	−0.2380	8.7840	−0.2090	8.7340	−0.2020
0.8850	9.0084	−0.2284	8.7793	−0.2043	8.7291	−0.1971
0.8900	8.9971	−0.2171	8.7735	−0.1985	8.7233	−0.1913
0.8950	8.9843	−0.2043	8.7668	−0.1918	8.7166	−0.1846
0.9000	8.9702	−0.1902	8.7592	−0.1842	8.7093	−0.1773
0.9050	8.9551	−0.1751	8.7508	−0.1758	8.7013	−0.1693
0.9100	8.9392	−0.1592	8.7417	−0.1667	8.6927	−0.1607
0.9150	8.9227	−0.1427	8.7320	−0.1570	8.6837	−0.1517
0.9200	8.9055	−0.1255	8.7216	−0.1466	8.6742	−0.1422
0.9250	8.8862	−0.1062	8.7098	−0.1348	8.6635	−0.1315
0.9300	8.8656	−0.0856	8.6969	−0.1219	8.6520	−0.1200
0.9350	8.8442	−0.0642	8.6834	−0.1084	8.6400	−0.1080
0.9400	8.8228	−0.0428	8.6696	−0.0946	8.6279	−0.0959
0.9450	8.8021	−0.0221	8.6562	−0.0812	8.6159	−0.0839
0.9500	8.7829	−0.0029	8.6434	−0.0684	8.6045	−0.0725
0.9550	8.7658	0.0142	8.6318	−0.0568	8.5940	−0.0620

Table B1 – *continued*

Phase	J	ΔJ	H	ΔH	K	ΔK
0.9600	8.7502	0.0298	8.6209	−0.0459	8.5841	−0.0521
0.9650	8.7357	0.0443	8.6105	−0.0355	8.5745	−0.0425
0.9700	8.7220	0.0580	8.6004	−0.0254	8.5652	−0.0332
0.9750	8.7089	0.0711	8.5905	−0.0155	8.5560	−0.0240
0.9800	8.6961	0.0839	8.5808	−0.0058	8.5470	−0.0150
0.9850	8.6836	0.0964	8.5712	0.0038	8.5381	−0.0061
0.9900	8.6710	0.1090	8.5616	0.0134	8.5292	0.0028
0.9950	8.6582	0.1218	8.5519	0.0231	8.5201	0.0119
1.0000	8.6450	0.1350	8.5420	0.0330	8.5110	0.0210

IR amplitudes are shown plotted against their corresponding V amplitudes in Fig. B2 with the following linear fits:

$$\Delta J = -0.015 + 0.450\,\Delta V, \tag{B3}$$

$$\Delta H = 0.111 + 0.206\,\Delta V, \tag{B4}$$

$$\Delta K = 0.176 + 0.125\,\Delta V. \tag{B5}$$

The J, H and K amplitudes of SW And are 0.395, 0.314 and 0.300, respectively. The corrections in Table B1 must therefore be multiplied by the following factors for a type *ab* variable with amplitude ΔV:

$$-0.038 + 1.139\,\Delta V \quad \text{for} \quad J, \tag{B6}$$

$$0.358 + 0.665\,\Delta V \quad \text{for} \quad H, \tag{B7}$$

$$0.594 + 0.417\,\Delta V \quad \text{for} \quad K. \tag{B8}$$

These corrections must be added to the observed magnitudes to obtain the mean magnitudes. In the case of RR*c* variables (which have quite low amplitudes), the above corrections can also be applied for the J magnitudes, while the K– $\langle K \rangle$ correction of Jones et al. (loc. cit.) can be applied to both the H and K magnitudes to get the mean magnitudes.

B1.4 The accuracy of these corrections

Table B2 compares the mean magnitudes $\langle J \rangle$, $\langle H \rangle$ and $\langle K_s \rangle$ derived from 2MASS data (Source 1) with those derived from the data of Fernley, Skillen & Burki (1993) (Source 2) and from unpublished H magnitudes of Kinman (Source 3). The largest discrepancies are for RZ Cep which is multiperiodic and has a double-peaked maximum (Cester & Todoran 1976). The second observation of RR Lyrae by Fernley et al. (1993) (indicated by an asterisk in Table B2) was taken near maximum light. RR Lyrae shows a Blazhko effect of varying period and so the large discrepancy between this and the other two observations is not surprising. If we neglect these observations, the mean differences in the sense (Fernley et al. *minus* 2MASS) are +0.006 ± 0.013, + 0.008 ± 0.015 and +0.008 ± 0.0015 mag for $\langle J \rangle$, $\langle H \rangle$ and $\langle K_s \rangle$, respectively. The mean difference (Kinman *minus* 2MASS) is -0.006 ± 0.006 for $\langle H \rangle$. These differences do not disagree with the small differences expected between observations made using the standards of Elias et al. (1982, 1983) as was the case of the Fernley et al. and the Kinman data and those on the 2MASS system (Carpenter 2001). It must be remembered that errors of as much as 0.2 mag can occur near the rising branch or with stars with varying light curves and/or ephemerides.

Table B2. Comparison of 2MASS mean magnitudes with those derived from other sources.

Star (1)	$\langle J \rangle$ (2)	$\langle H \rangle$ (3)	$\langle K_s \rangle$ (4)	Source (5)
SW And	8.807	8.578	8.506	(1)
		8.573		(3)
TU UMa	8.907	8.728	8.654	(1)
		8.714		(3)
BH Peg	9.345	9.085	9.041	(1)
	9.345	9.065	9.025	(2)
	9.395	9.055	9.009	(2)
		9.106		(3)
RR Lyr	6.739	6.511	6.462	(1)
	6.780	6.530	6.490	(2)
	6.930	6.670	6.650	(2)*
SV Eri	8.947	8.703	8.636	(1)
	8.915	8.672	8.658	(2)
	8.934	8.700	8.615	(2)
		8.682		(3)
RZ Cep	8.251	8.068	7.998	(1)
	8.350	8.270	8.160	(2)
	8.360	8.140	8.140	(2)
XZ Cyg	8.914	8.751	8.682	(1)
	8.970	8.790	8.770	(2)
	8.890	8.820	8.680	(2)
		8.730		(3)
DX Del	9.001	8.741	8.682	(1)
		8.736		(3)
X Ari	8.327	8.026	7.928	(1)
		8.030		(3)

This paper has been typeset from a TEX/LATEX file prepared by the author.